



# **UNIVERSIDAD DE INVESTIGACIÓN DE TECNOLOGÍA EXPERIMENTAL YACHAY**

**Escuela de Ciencias Físicas y Nanotecnología**

**TÍTULO: Study of the scalar power spectrum in the  
generalized Starobinsky model**

Trabajo de integración curricular presentado como requisito para  
la obtención  
del título de Físico

**Autor:**

Stefano Rafael Meza Anzules

**Tutor:**

Ph. D. Rojas Cely Clara

Urcuquí, marzo 2021

**SECRETARÍA GENERAL**  
**(Vicerrectorado Académico/Cancillería)**  
**ESCUELA DE CIENCIAS FÍSICAS Y NANOTECNOLOGÍA**  
**CARRERA DE FÍSICA**  
**ACTA DE DEFENSA No. UITEY-PHY-2021-00021-AD**

A los 7 días del mes de octubre de 2021, a las 12:30 horas, de manera virtual mediante videoconferencia, y ante el Tribunal Calificador, integrado por los docentes:

<b>Presidente Tribunal de Defensa</b>	Dra. PERALTA ARCIA, MAYRA ALEJANDRA DE JESUS , Ph.D.
<b>Miembro No Tutor</b>	Dr. COSENZA MICELI, MARIO GIUSEPPE , Ph.D.
<b>Tutor</b>	Dra. ROJAS CELY CLARA INES , Ph.D.

El(la) señor(ita) estudiante **MEZA ANZULES, STEFANO RAFAEL**, con cédula de identidad No. **1311845752**, de la **ESCUELA DE CIENCIAS FÍSICAS Y NANOTECNOLOGÍA**, de la Carrera de **FÍSICA**, aprobada por el Consejo de Educación Superior (CES), mediante Resolución **RPC-SO-39-No.456-2014**, realiza a través de videoconferencia, la sustentación de su trabajo de titulación denominado: **STUDY OF THE SCALAR POWER SPECTRUM IN THE GENERALIZED STAROBINSKY MODEL**, previa a la obtención del título de **FÍSICO/A**.

El citado trabajo de titulación, fue debidamente aprobado por el(los) docente(s):

<b>Tutor</b>	Dra. ROJAS CELY CLARA INES , Ph.D.
--------------	------------------------------------

Y recibió las observaciones de los otros miembros del Tribunal Calificador, las mismas que han sido incorporadas por el(la) estudiante.

Previamente cumplidos los requisitos legales y reglamentarios, el trabajo de titulación fue sustentado por el(la) estudiante y examinado por los miembros del Tribunal Calificador. Escuchada la sustentación del trabajo de titulación a través de videoconferencia, que integró la exposición de el(la) estudiante sobre el contenido de la misma y las preguntas formuladas por los miembros del Tribunal, se califica la sustentación del trabajo de titulación con las siguientes calificaciones:

Tipo	Docente	Calificación
Miembro Tribunal De Defensa	Dr. COSENZA MICELI, MARIO GIUSEPPE , Ph.D.	10,0
Tutor	Dra. ROJAS CELY CLARA INES , Ph.D.	9,8
Presidente Tribunal De Defensa	Dra. PERALTA ARCIA, MAYRA ALEJANDRA DE JESUS , Ph.D.	8,7

Lo que da un promedio de: **9.5 (Nueve punto Cinco)**, sobre 10 (diez), equivalente a: **APROBADO**

Para constancia de lo actuado, firman los miembros del Tribunal Calificador, el/la estudiante y el/la secretario ad-hoc.

*Certifico que en cumplimiento del Decreto Ejecutivo 1017 de 16 de marzo de 2020, la defensa de trabajo de titulación (o examen de grado modalidad teórico práctica) se realizó vía virtual, por lo que las firmas de los miembros del Tribunal de Defensa de Grado, constan en forma digital.*

**MEZA ANZULES, STEFANO RAFAEL**  
**Estudiante**

**Dra. PERALTA ARCIA, MAYRA ALEJANDRA DE JESUS , Ph.D.**  
**Presidente Tribunal de Defensa**

MAYRA  
 ALEJANDRA DE  
 JESUS PERALTA  
 ARCIA

Firmado digitalmente por  
 MAYRA ALEJANDRA DE  
 JESUS PERALTA ARCIA  
 Fecha: 2021.10.07 14:38:57  
 -05'00'

Dra. ROJAS CELY CLARA INES , Ph.D.  
**Tutor**

**CLARA INES**  
**ROJAS CELY** Firmado digitalmente por  
CLARA INES ROJAS CELY  
Fecha: 2021.10.07  
14:33:39 -05'00'

Dr. COSENZA MICELI, MARIO GIUSEPPE , Ph.D.  
**Miembro No Tutor**



Firmado electrónicamente por:  
**MARIO GIUSEPPE**  
**COSENZA MICELI**

CIFUENTES TAFUR, EVELYN CAROLINA  
**Secretario Ad-hoc**

**EVELYN**  
**CAROLINA**  
**CIFUENTES TAFUR** Firmado digitalmente  
por EVELYN CAROLINA  
CIFUENTES TAFUR  
Fecha: 2021.10.07  
13:45:45 -05'00'

## AUTORÍA

Yo, **STEFANO RAFAEL MEZA ANZULES**, con cédula de identidad 1311845752, declaro que las ideas, juicios, valoraciones, interpretaciones, consultas bibliográficas, definiciones y conceptualizaciones expuestas en el presente trabajo; así cómo, los procedimientos y herramientas utilizadas en la investigación, son de absoluta responsabilidad de el/la autora (a) del trabajo de integración curricular. Así mismo, me acojo a los reglamentos internos de la Universidad de Investigación de Tecnología Experimental Yachay.

Urcuquí, octubre 2021.



---

Stefano Rafael Meza Anzules

CI: 1311845752

## AUTORIZACIÓN DE PUBLICACIÓN

Yo, **STEFANO RAFAEL MEZA ANZULES**, con cédula de identidad 1311845752, cedo a la Universidad de Tecnología Experimental Yachay, los derechos de publicación de la presente obra, sin que deba haber un reconocimiento económico por este concepto. Declaro además que el texto del presente trabajo de titulación no podrá ser cedido a ninguna empresa editorial para su publicación u otros fines, sin contar previamente con la autorización escrita de la Universidad.

Asimismo, autorizo a la Universidad que realice la digitalización y publicación de este trabajo de integración curricular en el repositorio virtual, de conformidad a lo dispuesto en el Art. 144 de la Ley Orgánica de Educación Superior

Urcuquí, octubre 2021.



---

Stefano Rafael Meza Anzules  
CI: 1311845752

*To my mother Elsa, and to my father Rafael,*

*to my second parents Fernando, Carmita and Gabriel.*

## **Acknowledgements**

I want to express my eternal gratitude to my advisor, Ph.D. Clara Rojas. For all the support, guidance, and patience during this thesis. Thanks for giving me the opportunity to work by your side and for giving me a taste of how inflationary cosmology works. I really appreciate all the effort and dedication.

I desire to thank my family for all the support that they gave me during my undergraduate studies. There were several moments when I wanted to give up, and I stopped because you gave me the strength to keep advancing. All the goals I have achieved during this period is for you.

I would like to thank the AEFN-YT for giving me the opportunity of working in the communication department, where I could develop creative skills which now, I really appreciate. It was a pleasure to contribute to extracurricular activities which I consider particularly important for our University. Additionally, I would like to express my gratitude to the School of Physical Sciences and Nanotechnology, to its administrative component and to all the Professor who I had the opportunity to meet.

Yachay Tech give me a life full of experiences: from the English classes I took at the beginning of my career; during the common core where I met incredible people, who now are great professionals; from the extracurricular activities I had the opportunity to participate; from my roommates, which always made me day even better; and during all my specialization courses, where I met incredible friends. Thanks for all those great moments.

Specially, I want to express my gratitude to: Jhenson, who was the best person I could meet; Marcos, for being the best roomie in the world; Raul, for teaching me to never give up and to follow my dreams; and to Steven, who became my best friend during the last years of my career. Thanks for being there for me.

To all the students, professors, and people I had the opportunity to meet in Yachay Tech, I wish you the best of the world and hope one day we may see us again!

**Stefano Meza Anzules**

## Resumen

La teoría de la inflación cosmológica fue introducida para explicar los defectos dentro de la cosmología del Big Bang. Esta ha sido usada como la pieza clave para muchas teorías modernas de cosmología y gravedad. Depende principalmente de un potencial inflacionario que describe la expansión acelerada del universo, dando como resultado datos experimentales observados en la radiación de fondo de microondas. Dependiendo del potencial, valores ligeramente diferentes de los observables pueden ser calculados.

Para este manuscrito, se usó el potencial generalizado de Starobinsky  $V(\phi, p)$  con base en la aproximación slow-roll para obtener el espectro de potencia escalar, tensorial, sus respectivos índices espectrales y la proporción tensor-escalar. El principal valor calculado fue el espectro escalar de potencias, con un valor de  $\ln(10^{10}A_s) = 3.09376$  usando  $p = 1.004$ . Este valor muestra buena exactitud con respecto a la información experimental reportada por Planck 2018<sup>1</sup>.

**Keywords:** inflación cosmológica, espectro escalar de potencias, observables, análisis numérico, aproximación slow-roll, modelo inflacionario de Starobinsky.

## Abstract

The inflationary cosmological theory was introduced to explain the shortcomings in the Standard Big Bang Cosmology. It has been used as the backbone for many of the modern cosmological theories and gravity. It depends on an inflationary potential that describes the accelerated expansion, giving as a result, the current observed data in the CMB. According to the chosen potential, slightly different values of the observables can be computed.

For this manuscript, Generalized Starobinsky Potential  $V(\phi, p)$  was used in the slow-roll approximation for obtaining the scalar and tensor power spectrum, their spectral index, and the scalar-to-tensor ratio. The main computed value was the scalar power spectrum  $\ln(10^{10}A_s) = 3.09376$  by setting  $p = 1.004$ . This value is in good accuracy with the experimental data reported in Planck 2018.

**Keywords:** cosmological inflation, scalar power spectrum, cosmological observables, numerical analysis, slow roll, Starobinsky inflationary model.

# Contents

<b>List of Figures</b>	<b>xii</b>
<b>List of Tables</b>	<b>xiii</b>
<b>1 Introduction</b>	<b>1</b>
1.1 Standard Big Bang Cosmology . . . . .	1
1.1.1 Equation of state . . . . .	3
1.2 General and Specific Objectives . . . . .	3
<b>2 Theoretical Background</b>	<b>5</b>
2.1 Shortcomings in the SBB cosmology . . . . .	5
2.1.1 Flatness Problem . . . . .	5
2.1.2 Horizon problem . . . . .	6
2.2 Inflationary Cosmology . . . . .	8
2.2.1 Horizon problem revisited . . . . .	8
2.2.2 Flatness problem revisited . . . . .	9
2.3 Scalar field . . . . .	9
2.3.1 Slow-roll approximation . . . . .	10
2.3.2 Slow-roll parameters . . . . .	11
2.4 Cosmological perturbation Theory . . . . .	12
2.4.1 Inflaton perturbation theory . . . . .	12
2.4.2 Perturbation of a Massless field in De Sitter . . . . .	13
2.4.3 Power Spectrum . . . . .	15
2.4.4 Massless scalar field in quasi-de-Sitter . . . . .	16
2.4.5 Scalar and Tensorial modes . . . . .	17
<b>3 Methodology</b>	<b>21</b>
3.1 Starobinsky Inflation . . . . .	21

3.1.1	Generalized Starobinsky Potential . . . . .	23
3.1.2	Domain of the p-value . . . . .	24
3.2	Solving Friedman slow-roll equations . . . . .	24
3.2.1	Horizon Crossing . . . . .	27
3.3	Cosmological Observables . . . . .	27
3.3.1	Parameters . . . . .	27
3.3.2	Experimental observations . . . . .	28
<b>4</b>	<b>Results &amp; Discussion</b>	<b>31</b>
4.1	Scalar field and Scale factor . . . . .	31
4.2	Scalar power spectrum and spectral index . . . . .	32
4.3	Tensor Power Spectrum, Spectral Index and Tensor-to-scalar Ratio . . . . .	35
<b>5</b>	<b>Conclusions &amp; Outlook</b>	<b>39</b>
	<b>Bibliography</b>	<b>41</b>

# List of Figures

2.1	General representation of an inflationary potential. Inflation occurs when kinetic energy is much smaller than the potential of the field. Inflation ends at $\phi_{end}$ when the kinetic term is comparable with the potential. CMB fluctuations $\phi_{CMB}$ are created before inflation ends at 60 e-folds. Finally, reheating occurs, and energy density is converted into radiation <sup>2</sup> . . . . .	10
3.1	Generalized Starobinsky Potential for several values of $p$ . <i>Left</i> : Potential evaluated at $p \geq 1$ , black arrow represents the growth of a maximum. <i>Right</i> : Potential evaluated at $p \leq 1$ . The black arrow represents how only one vacuum is generated. Fig. 3.1a represents the vacuum at the origin while Fig 3.1b represents a possible vacuum when $\phi/M_{pl}$ tends to positive infinity. . . . .	24
3.2	Generalized Starobinsky Potential. Warm colors represent small values of $p$ while cold colors symbolize large values of $p$ . For $p = 1$ , denoted by the black line, it represents the well-known Starobinsky Potential. . . . .	25
4.1	<i>Left</i> : Time evolution of the scalar field during the inflationary epoch. <i>Right</i> : Time evolution of the scale factor. For both graphs, different values of $p$ are displayed. . . . .	32
4.2	Behaviour of the cosmological observables with respect of different values of $p$ at $k = 0.05$ . <i>Left</i> : $\ln(10^{10}A_S)$ . <i>Right</i> : Scalar spectral index. . . . .	33
4.3	Deeper view of the $\ln(10^{10}A_S)$ from $p = 1.0003$ to $p = 1.0007$ at $k = 0.05$ . . . . .	34
4.4	Dynamics of the cosmological observables for $p = 1.0004$ at different values of $k$ . <i>Left</i> : Scalar Power Spectrum. <i>Right</i> : Scalar Spectral Index. Red dots describes the values at $k = 0.05$ . . . . .	35
4.5	Behaviour of the cosmological observables for different values of $p$ at $k = 0.05$ . <i>Left</i> : tensor power spectrum. <i>Right</i> : tensor-to-scalar ratio. <i>Bottom</i> : tensor Spectral Index. . . . .	36
4.6	Dynamics of the cosmological observables for $p = 1.0004$ at different values of $k$ . <i>Left</i> : Tensor Power Spectrum. <i>Right</i> : Tensor-to-scalar ratio. <i>Bottom</i> : Tensor Spectral Index. Red dots describes the values at $k = 0.05$ . . . . .	37



# List of Tables

1.1	Behaviour of the energy density and scale factor for different epochs of the universe <sup>3</sup> . . . . .	3
3.1	Experimental values of the Cosmological observables. $A_S$ is the scalar power spectrum, $n_S$ is its spectral index, $r$ is defined as the scalar-to-tensor ratio and the $\ln 10^{10} A_S$ is a more convenient way for describing the scalar power spectrum. Those values are taken from Planck 2018. . . . .	29
4.1	Initial $\phi_0$ and final $\phi_f$ values of the scalar field in the inflationary epoch for different values of $p$ . . .	31
4.2	Computed values of the cosmological observables: (a) Scalar Power Spectrum $A_s$ , (b) $\ln(10^{10} A_s)$ , (c) and its spectral index ( $n_s$ ). . . . .	33
4.3	Computed values of the cosmological observables $A_s$ and $\ln(10^{10} A_s)$ from $p = 0.0003$ to $p = 0.0007$ at $k = 0.05$ . . . . .	33
4.4	Computed values of the cosmological observables $P_T$ , $n_T$ and $r$ for several values of $p$ at $k = 0.05$ . .	35
4.5	Set of cosmological observables using computed at $p = 1.004$ by using the Generalized Starobinsky Potential and the experimental values reported in Planck 2018. . . . .	38



# Chapter 1

## Introduction

### 1.1 Standard Big Bang Cosmology

Assuming a homogeneous and isotropic universe on large scales, it is possible to use the Friedmann-Robertson-Walker (FRW) metric<sup>4</sup>:

$$ds^2 = dt^2 - a(t) \left[ \frac{dr^2}{\sqrt{1 - Kr^2}} + r^2 d\theta^2 + r^2 \sin(\theta)^2 d\phi^2 \right], \quad (1.1)$$

where  $a(t)$  represents the scale factor, which states how space is expanding.  $K$  is known as the curvature parameter: if  $K = 1$ , universe is positively curved, for  $K = -1$  universe is negatively curved, and for  $K = 0$  the universe is flat. Einstein equations relate the scale factor expression with the energy distribution in the universe. The Einstein tensor can be obtained from the metric and can be defined as:

$$G_{\mu\nu} = 8\pi G_N T_{\mu\nu}, \quad (1.2)$$

$$G_{\mu\nu} = R_{\mu\nu} - \frac{1}{2} R g_{\mu\nu}, \quad (1.3)$$

where  $R_{\mu\nu}$  is the Ricci tensor,  $R$  is the Ricci curvature scalar.  $T_{\mu\nu}$  is the energy-momentum tensor of matter,  $G_N$  is the Newtonian constant. For obtaining the equations of motion associated with the expansion of the universe, it is necessary to compute the Ricci tensor. Their non-vanishing components are:

$$R_{00} = -3\frac{\ddot{a}}{a}, \quad (1.4)$$

$$R_{ij} = \left[ \frac{\ddot{a}}{a} + 2\left(\frac{\dot{a}}{a}\right)^2 + 2\frac{K}{a^2} \right] g_{ij}. \quad (1.5)$$

By taking  $g_j^i = \delta_{ij}$ , the non-vanishing components of the Einstein tensor are:

$$G_0^0 = 3 \left[ \left( \frac{\dot{a}}{a} \right)^2 + \frac{K}{a^2} \right], \quad (1.6)$$

$$G_j^i = \left[ 2 \frac{\ddot{a}}{a} + \left( \frac{\dot{a}}{a} \right)^2 + \frac{K}{a^2} \right] \delta_{ij}. \quad (1.7)$$

For this case, it is necessary to assume that the energy-momentum tensor has a similar structure to the metric. The related fluid will be considered an ideal one with energy density  $\rho$  and pressure  $p$ . Then, the matrix takes the form of:

$$T_\nu^\mu = \begin{pmatrix} \rho & 0 & 0 & 0 \\ 0 & -p & 0 & 0 \\ 0 & 0 & -p & 0 \\ 0 & 0 & 0 & -p \end{pmatrix}. \quad (1.8)$$

By replacing equations (1.2), (1.6), (1.7) into the diagonal components of the energy-momentum tensor (1.8), it is possible to obtain the following relation:

$$\left[ \left( \frac{\dot{a}}{a} \right)^2 + \frac{K}{a^2} \right] = \frac{8\pi G_N}{3} \rho, \quad (1.9)$$

$$\left[ 2 \frac{\ddot{a}}{a} + \left( \frac{\dot{a}}{a} \right)^2 + \frac{K}{a^2} \right] = -8\pi G_N p. \quad (1.10)$$

By summing equations (1.9) and (1.10) an expression for the cosmic acceleration<sup>5</sup> is obtained as follows:

$$\frac{\ddot{a}}{a} = -\frac{4\pi G_N}{3} (\rho + 3p). \quad (1.11)$$

Another practical relation can be obtained by computing the derivative of equation (1.9) as follows:

$$\frac{8\pi G_N}{3} \dot{\rho} = \left( \frac{\dot{a}}{a} \right) \left[ 2 \frac{\ddot{a}}{a} - 2 \left( \frac{\dot{a}}{a} \right)^2 - 2 \frac{K}{a^2} \right], \quad (1.12)$$

therefore, it is possible to obtain:

$$\dot{\rho} = -3 \left( \frac{\dot{a}}{a} \right) (\rho + p). \quad (1.13)$$

Equation (1.13) is equivalent to the energy conservation equation. By defining:

$$H = \frac{\dot{a}}{a}, \quad (1.14)$$

equation (1.9) and (1.13) take the following form:

$$H^2 + \frac{K}{a^2} = \frac{8\pi G_N}{3}\rho, \quad (1.15)$$

$$\dot{\rho} = -3H(\rho + p). \quad (1.16)$$

Equation (1.15) is known as the **Friedman equation**, and equation (1.16) is known as the **energy conservation equation**.

### 1.1.1 Equation of state

The universe is an ideal fluid which fulfills the following relation:

$$p = w\rho. \quad (1.17)$$

By replacing equation (1.17) in (1.16):

$$\frac{d\rho}{\rho} = -3(1+w)\frac{da}{a}, \quad (1.18)$$

where it is possible to analyze the scale factor dependence of the fluid during different epochs of the universe<sup>6</sup>. Furthermore, by setting  $K = 0$  in equation (1.15) it may be also analyzed the time dependence of the scale factor. The obtained results can be seen in Table 2.1.

epoch	$w$	$\rho(a)$	$a(t)$
<b>Radiation-dominated</b>	1/3	$\propto a^{-4}$	$\propto t^{1/2}$
<b>Cosmological Constant</b>	-1	$\propto a^0$	$\propto e^{\sqrt{\frac{8}{3}}t}$
<b>Matter-dominated</b>	-1/3	$\propto a^{-3}$	$\propto t^{2/3}$

**Table 1.1:** Behaviour of the energy density and scale factor for different epochs of the universe<sup>3</sup>.

For matter-epoch, if  $w > -1/3$  the expansion of the universe is accelerating while for  $w < -1/3$  it is decelerating.

## 1.2 General and Specific Objectives

- Based on the literature, demonstrate the equations of the Cosmological Perturbation Theory in the Inflationary epoch.
  - Using the Einstein-Hilbert Action, calculate the equation for the Scalar Power spectrum and the Tensor Power Spectrum.
- Identify the value of the free parameter  $p$  in the Generalized Starobinsky Potential which allows a high accuracy with the observable data exposed by Planck 2018.

- Compute the scalar power spectrum and its running index for different values of  $p$ . Then, make a comparison of the obtained values with the experimental data in order to analyze the precision of the results.
- Using the previously obtained  $p$ -value, compute the whole set of the parameters. Those include: scalar power spectrum, tensor power spectrum, its running index, and the scalar to tensor ratio.

In section 2 it is described all the theoretical background of the thesis, obtaining the Friedman Equations, the Einstein-Hilbert action and the Classical and Quantum Perturbation theory. In section 3 using the previously expressions; slow roll parameters, power spectrum and their corresponding running indexes will be computed in terms of the Generalized Starobinsky Potential, which is the key of the manuscript. Finally, in section 4 the theoretical values of the scalar power spectrum and its running index will be compared with the ones obtained by Planck 2018. An analysis will be done in order to analyze which is the best value of the free parameter  $p$ . Consequently, the rest of the cosmological values will be plotted and computed with the final  $p$ -value.

# Chapter 2

## Theoretical Background

### 2.1 Shortcomings in the SBB cosmology

The following discussion was developed by Brawer<sup>7</sup>.

#### 2.1.1 Flatness Problem

The flatness problem arises from the observational constraints on omega  $\Omega$ , a dimensionless parameter that relates the universe's actual mass density with the critical mass density. A universe with  $\Omega = 1$  is globally flat. First observations demonstrated that this value is between  $0.1 < \Omega_o < 2$ . Therefore, this value needed to be around  $10^{-15}$  during the Big Bang for having this value. This is known as a fine-tuning problem; thus, it is a sporadic case. A mathematical demonstration can be shown as follows: As it was said,  $\omega$  can be described by the following relation:

$$\Omega = \frac{\rho}{\rho_c}, \quad (2.1)$$

$$\rho_c = \frac{3H^2}{8\pi G_N}. \quad (2.2)$$

In which the critical density value comes from equation (1.15) by setting  $K = 0$ . For obtaining the value of  $\omega$  at the Big Bang epoch, it is needed to evaluate the transition from the radiation-dominated epoch to the matter-dominated epoch. This will be expressed as  $\rho_{rad}/\rho_{mat} = 1$  By using the expressions in the table 2.1, the following equation is obtained:

$$\frac{\rho_{rad}(t)}{\rho_{mat}(t)} = \frac{\rho_{rad}(t_o)}{\rho_{mat}(t_o)} \left( \frac{a(t_o)}{a(t)} \right). \quad (2.3)$$

For matter-dominated epoch:

$$\frac{\rho_{rad}(t)}{\rho_{mat}(t)} = 10^{-4} \left( \frac{t_o}{t} \right)^{2/3}. \quad (2.4)$$

By taking the universe's age as  $t_o$  equals 13 billion years, then the transition time  $t_T$  is about 13000 years. Nowadays, its actual value is approximately:

$$\left| \frac{\Omega_o - 1}{\Omega_o} \right| < 10. \quad (2.5)$$

During matter-dominated epoch:

$$\left| \frac{\Omega - 1}{\Omega} \right| = \left( \frac{t}{t_o} \right)^{2/3} \left( \frac{\Omega_o - 1}{\Omega_o} \right). \quad (2.6)$$

Therefore, the transition between radiation-dominated and matter-dominated epochs is:

$$\left| \frac{\Omega_T - 1}{\Omega_T} \right| = 10^{-4} \left( \frac{\Omega_o - 1}{\Omega_o} \right). \quad (2.7)$$

Finally, in radiation-dominated era, this ratio scales directly with  $t$ . At  $t=1$ , which was the time when nucleosynthesis took place:

$$\left| \frac{\Omega_N - 1}{\Omega_N} \right| = 2 \times 10^{-16} \left( \frac{\Omega_o - 1}{\Omega_o} \right), \quad (2.8)$$

$$|\Omega - 1|_{t=1s} < 10^{-15}. \quad (2.9)$$

As it can be seen, to have the actual values of omega, its initial value needed to be about  $10^{-15}$ .

### 2.1.2 Horizon problem

Horizon problem arises from the observed uniformity of the CMB. Experimental observations found that the radiation temperature is isotropic to better than 1 part in  $10^4$ . Analyzing the time of the emission and considering regions in opposite directions, those were significantly outside their horizons. Thus, any information exchange between photons from each region could not be possible for reaching thermal equilibrium. For understanding this problem, consider a photon which propagates along the world lines such that:

$$ds^2 = 0. \quad (2.10)$$

By considering the light emitted by one comoving observer at  $r_e$  at  $t_e$  and a receiver at  $r_o$  and  $t_o$ . The time propagation is:

$$\int_{t_e}^{t_o} \frac{cdt}{a(t)} = \int_o^{r_e} \frac{dr}{\sqrt{1 - Kr^2}}. \quad (2.11)$$

If the light frequency is  $\nu$  and  $\Delta t_e = 1/\nu_e$ , then equation (2.11) will describe the trajectory of the final wavefront, the crest of the second wavefront is described by:

$$\int_{t_e + \Delta t_e}^{t_o + \Delta t_o} \frac{cdt}{a(t)} = \int_o^{r_e} \frac{dr}{\sqrt{1 - Kr^2}}. \quad (2.12)$$

By using equations (2.11) and (2.12) and considering  $a(t - \Delta t) \approx a(t)$ :

$$\frac{\Delta t_o}{\Delta t_e} = \frac{a(t_e)}{a(t_o)} \rightarrow \frac{\lambda_o}{\lambda_e} = \frac{a(t_e)}{a(t_o)}. \quad (2.13)$$

The red-shift parameter  $z$  is defined as:

$$1 + z = \frac{\lambda_o}{\lambda_e} = \frac{a(t_o)}{a(t_e)}, \quad (2.14)$$

where it expresses the amount of expansion of the universe since the light was emitted. If  $z = 1$ , then the universe has doubled its size. The proper distance is defined as:

$$d_{prop} = a(t_o) \int_{t_e}^{t_o} \frac{cdt}{a(t)}. \quad (2.15)$$

Given a emission time  $t_e$ , there exists a region of comoving space  $r \leq r_c$  such that signals outside the region could not reached  $r = 0$  by time  $t_o$ . Then:

$$a(t) = \int_0^t \frac{cdt'}{a(t')}, \quad (2.16)$$

represents how far a signal could have traveled from  $t = 0$ . If it converges, is is known as the particle horizon. Another useful relation is:

$$d_h(t) = a(t) \int_0^t \frac{cdt'}{a(t')} = a(t) \int_0^{r_h} \frac{dr}{\sqrt{1 - Kr^2}}, \quad (2.17)$$

where  $d_h$  is the proper distance and  $r_h$  is the radial comoving coordinate. By setting  $K = 0$ , the previous equation may be solved:

$$d_h(t) = t^{1/2} \int_0^t \frac{cdt'}{t^{1/2}} = 2ct, \quad (2.18)$$

where this is for radiation-dominated epoch and:

$$d_h(t) = 3ct, \quad (2.19)$$

is for matter dominated epoch. Furthermore, CMB radiation came uniformly from every direction of the space, then:

$$d_{CMB}(t_e) = a(t_e) \int_{t_e}^{t_o} \frac{cdt}{a(t)}, \quad (2.20)$$

where  $d_{CMB}$  is the distance of the source of the measured radiation. At  $t_e$  sources come from opposite directions so:

$$d_{sep} = 2d_{CMB}(t_e), \quad (2.21)$$

where  $d_{sep}$  is the distance of sky and the size of the horizon at the time of emission was:

$$d_h(t_e) = a(t_e) \int_0^{t_e} \frac{cdt}{a(t)}. \quad (2.22)$$

Therefore, it is possible to obtain a relation between the separation distance and the horizon distance to analyze how far they were at the emission. Then:

$$\frac{d_{sep}(t_e)}{d_h(t_e)} = \frac{2 \int_{t_e}^{t_o} \frac{cdt}{a}}{\int_0^{t_e} \frac{cdt}{a}}, \quad (2.23)$$

and by setting  $K = 0$ :

$$\frac{d_{sep}(t_e)}{d_h(t_e)} = 2 \left[ (1+z)^{1/2} - 1 \right], \quad (2.24)$$

the CMB was emitted at  $z = 1500$ , then the separation distance was about 80 times larger than the horizon distance at the light emission. Then, it was impossible that those photons had the same temperature if they were never in thermal equilibrium.

## 2.2 Inflationary Cosmology

Inflation is defined as a brief period in which the expanding universe's scalar factor is an exponential equation. This was a rapid process from about  $10^{-35}$  to  $10^{-32}$  after the Big Bang. This was introduced for solving the Flatness and the Horizon problem. Nevertheless, better applications had been found, such as the explanation of the density perturbations presented in the CMB. This will be analyzed later. Equations for inflation can be obtained as follows. First, recall equation (1.15):

$$\left( \frac{\dot{a}}{a} \right)^2 = \frac{8\pi G_N \rho}{3} - \frac{k^2}{a^2}, \quad (2.25)$$

and assume that the energy density  $\rho$  is constant and that curvature constant  $K$  is negligible, then the Friedman equation for the inflationary epoch is:

$$\dot{a}^2 = \frac{8\pi G_N \rho}{3} a^2, \quad (2.26)$$

where the scale factor is defined as:

$$a(t) = C e^{H_o t}, \quad (2.27)$$

by taking:

$$H_o = \sqrt{\frac{8\pi G_N \rho}{3}}. \quad (2.28)$$

It is said that inflation lasts for  $10^{-32} s$ , then the scale factor is taken to be about  $e^{100}$  and its scale factor takes a value about  $10^{50}$ .

### 2.2.1 Horizon problem revisited

Compute the horizon distance for the new scale factor:

$$d_H(t_{end}) = a(t_{end}) \int_{t_{start}}^{t_{end}} \frac{cdt}{a(t)}, \quad (2.29)$$

where  $t_{end}$  and  $t_{start}$  were the time where inflation end and started respectively. Then:

$$d_H(t_{end}) = \frac{c e^{H(t_{end})}}{H}. \quad (2.30)$$

By using the values defined previously:

$$d_H(t_{end}) = \frac{1}{H} c e^{100} \approx 10^{19} cm. \quad (2.31)$$

At the present, the radius of the observable universe was computed from (2.19) giving  $10^{28}$  cm. At the end of the inflationary expansion, the scale factor was  $10^{-27}$ . Then, its physical size was about 10 cm. This value falls inside the horizon distance calculated previously. This means that regions from the space were in contact, thus thermal equilibrium took place and then in inflation those blow up for occupying huge regions of space.

### 2.2.2 Flatness problem revisited

By recalling the following equation:

$$\frac{\Omega - 1}{\Omega} = \frac{3k}{8\pi G_N \rho a^2}, \quad (2.32)$$

where all values are constant in the inflationary epoch except for the scale factor which scales up to  $e^{50}$ . Then, the denominator of the R.H.S. will have a factor of  $10^{100}$ . This means that after inflation,  $\Omega$  will be very close to 1.

## 2.3 Scalar field

Having a large cosmological constant is trouble for the cosmology because the energy density does not decay in the inflation. Therefore, a large cosmological constant does not match with the experimental observations. To solve this, it is needed to introduce a fluid capable of mimic a sizeable cosmological constant during this period. for some time. The solution for this is a scalar field.

The simplest case of a single real scalar can be obtained with the Lagrangian<sup>8</sup>:

$$\mathcal{L} = \frac{1}{2} \partial^\mu \phi \partial_\mu \phi - V(\phi) = \frac{1}{2} (\dot{\phi}^2 - \nabla^2 \phi - V(\phi)). \quad (2.33)$$

By using Noether's theorem, the energy-momentum tensor can be related with the field:

$$T^{\mu\nu} = \partial^\mu \phi \partial^\nu \phi - g^{\mu\nu} \mathcal{L}, \quad (2.34)$$

where the pressure and the energy density of this new fluid are expressed by:

$$\rho = T^{00} = \frac{1}{2} \dot{\phi}^2 + V(\phi) + \frac{1}{2} (\nabla \phi)^2, \quad (2.35)$$

$$p = T^{11} = \frac{1}{2} \dot{\phi}^2 - V(\phi) - \frac{1}{6} (\nabla \phi)^2. \quad (2.36)$$

By replacing the previously obtained equations in (1.15) and (1.16) it is possible to obtain:

$$H^2 = \frac{1}{3M_{pl}^2} \left( V(\phi) + \frac{1}{2} \dot{\phi}^2 \right), \quad (2.37)$$

$$\ddot{\phi} + 3H\dot{\phi} = -V'(\phi), \quad (2.38)$$

where those are the equation of motion for the scalar field in the inflationary epoch and the reduced Planck mass is:

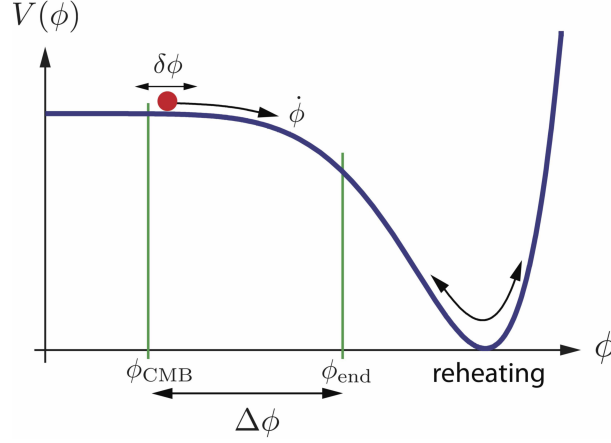


**Figure 2.1:** General representation of an inflationary potential. Inflation occurs when kinetic energy is much smaller than the potential of the field. Inflation ends at  $\phi_{end}$  when the kinetic term is comparable with the potential. CMB fluctuations  $\phi_{CMB}$  are created before inflation ends at 60 e-folds. Finally, reheating occurs, and energy density is converted into radiation<sup>2</sup>.

$$M_{pl} = \sqrt{\frac{1}{8\pi G_N}}. \quad (2.39)$$

### 2.3.1 Slow-roll approximation

Inflation must be finite, and thus it is required to end up after some brief period of time. At this point, all its energy is converted into matter/radiation. This is called reheating. To explain this, it is possible to have two models: The first one considers a cosmological constant, which is the principal actor that generates the accelerated expansion, and by imposing that it may decay, it can fulfill the reheating process. The second alternative is much more accurate by defining scalar fields with the property to behave as a dynamical cosmological constant.

Therefore, as shown in Figure 2.1, it is convenient to start with a nearly flat potential:  $\dot{\phi}^2 \ll V(\phi)$ , which will behave as a false vacuum. After some evolution, the scalar field is slowly rolling down:  $|\ddot{\phi}| \ll |V'(\phi)|$  until it reaches the true vacuum. This is the reason why it is called slow-roll<sup>9</sup>. This inflationary regime occurs when the kinetic term can be neglected, and the potential dominates the whole expression. When both quantities become comparable, reheating process occurs<sup>3</sup>. It is verifiable that the slope and the curvature of the potential must be small [ $V'(\phi), V''(\phi) \ll V(\phi)$ ]. Once these conditions are fulfilled, equations (2.37) and (2.38) may be rewrite as:

$$H^2 \simeq \frac{V}{3M_{pl}^2}, \quad (2.40)$$

$$3H\dot{\phi} \simeq -V', \quad (2.41)$$

### 2.3.2 Slow-roll parameters

It is imperative to introduce the potential slow-roll parameters  $\epsilon$  and  $\delta$ . In the Einstein frame those have the following structure:

$$\epsilon_v = \frac{M_{pl}^2}{2} \left( \frac{V'(\phi)}{V(\phi)} \right)^2, \quad (2.42)$$

$$\delta_v = M_{pl}^2 \left( \frac{V''(\phi)}{V(\phi)} \right). \quad (2.43)$$

And equations (2.40) and (2.41) are in agreement with slow-roll if and only if:

$$\epsilon_v(\phi) \ll 1, \quad (2.44)$$

$$|\delta_v(\phi)| \ll 1. \quad (2.45)$$

A physical meaning can be seen for the  $\epsilon_v$  as follows:

$$\frac{\ddot{a}}{a} > 0 \rightarrow \epsilon_v(\phi) < 1. \quad (2.46)$$

Hence, inflation ends when the following equation is reached:

$$\epsilon(\phi_f) = 1. \quad (2.47)$$

Finally, another useful parameter for describing inflation is the e-fold number  $N$ . It can be calculated by dividing the scale factor at the beginning and at the end of the expansion. For convenience, it is written in terms of its logarithm as it may be seen:

$$N = \ln \frac{a(t_f)}{a(t_i)}. \quad (2.48)$$

And a more general expression is:

$$N = \sqrt{\frac{1}{2M_{pl}^2}} \int_{\phi_i}^{\phi_f} \frac{V(\phi)}{V'(\phi)} d\phi. \quad (2.49)$$

## 2.4 Cosmological perturbation Theory

The universe was made almost uniformly by a primordial inflationary stage. It was originated from small seed perturbations, which gave birth to all the structures that may be observed. Those seeds started to grow by gravitational instabilities in the matter-dominated era and formed complex matter structures.

The Cosmic Microwave Background anisotropies measurements confirmed the presence of those primordial inflationary seeds, and one of the most accepted hypotheses is that those come from the inflationary epoch. Nevertheless, the main goal of inflation was to explain the shortcomings of the Standard Big Bang theory, such as horizon and flatness. However, the essential characteristic is that it generates the spectra of density perturbations and gravitational waves.

At the end of inflation, the matter-dominated era started, and fluctuations re-enter because the Hubble radius increased faster than the scale factor. The small fluctuations in inflation are related to the space-time metric fluctuations, the energy-momentum tensor, and the Einstein field equation. By taking the wavelength of the perturbations as  $\lambda$ , it is said that those grew exponentially and leave soon of the Hubble radius when  $\lambda > H^{-1}$ . At super-Hubble scales, curvature fluctuations were frozen, therefore those can be considered as classical and their amplitude remains constant. Once they reenter the horizon, curvature perturbation gives rise to matter and temperature perturbation and give that forms the structures of today.

For analyzing the cosmological perturbation theory, it will be divided into two sections: First, the simplest case will be analyzed which is the quantum fluctuations of a generic scalar field. Then, those results will be used to compute quantum fluctuations in which metric perturbations and consequently, tensor will be now considered.

### 2.4.1 Inflaton perturbation theory

The following theory was developed by Alexander Riotto<sup>10</sup>. The Lagrangian of the inflaton is written as follows:

$$S[\phi] = - \int d^4x \sqrt{-g} \left[ \frac{1}{2} g^{\mu\nu} \partial_\mu \phi \partial_\nu \phi + V(\phi) \right], \quad (2.50)$$

where its equation of motion in function of time and  $x$  is defined as:

$$\ddot{\phi} + 3H\dot{\phi} - \frac{\nabla^2 \phi}{a^2} + V'(\phi) = 0. \quad (2.51)$$

By splitting the inflaton and writing up to first order (linear perturbation):

$$\phi(\vec{x}, t) = \phi_o(t) + \delta\phi(\vec{x}, t). \quad (2.52)$$

Now, construct both terms in equation (2.52):

$$\ddot{\phi}_o + 3H\dot{\phi}_o + V'(\phi_o) = 0, \quad (2.53)$$

$$\delta\ddot{\phi} + 3H\delta\dot{\phi} - \frac{\nabla^2 \delta\phi}{a^2} + V''\delta\phi = 0. \quad (2.54)$$

Assume perturbations of very long wavelength, larger than the Hubble radius of inflation  $\lambda \gg \gg H^{-1}$ , therefore the gradient of equation (2.54) can be neglected. By taking the time derivative of equation (2.53), and assuming  $H$  constant at first approximation:

$$\ddot{\phi}_o + 3H\dot{\phi}_o + V''(\phi_o) = 0. \quad (2.55)$$

For this case, equation (2.55) is equivalent to (2.54) without the gradient, and it reduces to:  $\dot{\phi}_o \approx \delta\dot{\phi}$ . Therefore, at very long wavelengths the:

$$\delta\phi(\vec{x}, t) = -\dot{\phi}_o \tau(\vec{x}), \quad (2.56)$$

and equation (2.56) can be written as:

$$\phi(\vec{x}, t) = \phi_o(t - \tau(\vec{x})). \quad (2.57)$$

The universe has the same value of the inflaton up to small fluctuations.

### 2.4.2 Perturbation of a Massless field in De Sitter

The Lagrangian of an arbitrary massless scalar field is:

$$\chi[\vec{x}, t] \rightarrow S[\chi] = -\frac{1}{2} \int d^4x \sqrt{-g} (g^{\mu\nu} \partial_\mu \chi \partial_\nu \chi), \quad (2.58)$$

where the potential term is zero and the kinetic term is the only one in the action. The equation of motion can be defined as:

$$\ddot{\chi} + 3H\dot{\chi} - \frac{\nabla^2 \chi}{a^2} = 0. \quad (2.59)$$

By expanding the scalar field  $\chi$  in Fourier modes:

$$\chi(\vec{x}, t) = \int \frac{d^3k}{(2\pi)^{3/2}} e^{i\vec{k}\cdot\vec{x}} \chi_k(t). \quad (2.60)$$

By applying equation (2.60) in (2.59):

$$\ddot{\chi}_k + 3H\dot{\chi}_k + \frac{k^2}{a^2} \chi_k = 0. \quad (2.61)$$

During inflation and a the Sitter period, Hubble radius is assumed to be constant. Therefore it is possible to have two periods of interaction.

- **Wavelengths inside the Hubble radius:** for this case, the following relation is fulfilled:

$$\lambda = \frac{a}{k} \rightarrow \frac{k}{aH} \gg 1, \quad (2.62)$$

therefore, we can neglect the  $3H\dot{\chi}_k$  in equation (2.59) Then, the equation of motion can be written as:

$$\ddot{\chi}_k + \frac{k^2}{a^2} \chi_k = 0. \quad (2.63)$$

This is the equation of an oscillator with a time dependent frequency. The solution will have the form of an propagating wave.

- **Wavelengths outside the Hubble radius:** in this regime, the relation is the following one:

$$\lambda = \frac{a}{k} \rightarrow \frac{k}{aH} \ll 1, \quad (2.64)$$

and the  $\frac{k^2}{a^2}\chi_k$  is neglected. The equation (2.59) reduces to:

$$\ddot{\chi} + 3H\dot{\chi} = 0. \quad (2.65)$$

The solution for this equation is a constant. Therefore, for super-Hubble regime, the wavelength will remain frozen.

For obtaining an accurate result, it is necessary to solve explicitly the equations of motion. One possible path for doing this is by introducing the conformal time. This is defined as:

$$d\tau = \frac{dt}{a}, \quad (2.66)$$

and by replacing its value in the FLRM metric:

$$ds^2 = a^2(\tau) \left[ -d\tau^2 + (d\vec{x})^2 \right]. \quad (2.67)$$

Which is said to be conformal to Minkowski due to its structure. Consequently, the scale factor can be rewrite as:

$$a = -\frac{1}{H\tau}. \quad (2.68)$$

For  $\tau = 0$  inflation ends and for  $\tau < 0$  inflation was taking place. By plugging these equations into the action of a massless field (2.58):

$$S = \int d^4x a^2 \left[ \frac{1}{2} \dot{\chi}^2 - \frac{(\nabla\chi)^2}{2} \right], \quad (2.69)$$

where the time derivative is taken with respect of  $\tau$ . By considering the new scalar field transformation:

$$\chi(\vec{x}, t) = \frac{\sigma(\vec{x}, t)}{a}, \quad (2.70)$$

the new action is rewritten as:

$$S[\sigma] = \frac{1}{2} \int d^4x \left[ (\sigma')^2 - (\nabla\sigma)^2 + \underbrace{\sigma^2 \frac{a''}{a}}_{mass} \right]. \quad (2.71)$$

Performing a Fourier transformation 2.60 in (2.71) it is possible to obtain the following equation of motion:

$$\sigma_k'' + \left( k^2 - \frac{a''}{a} \right) \sigma_k = 0. \quad (2.72)$$

The same analysis must be performed to compute the analytical solutions of the perturbations:

- **Wavelength inside the Hubble radius:** the following condition must be fulfilled:

$$-k\tau \gg 1, \quad (2.73)$$

therefore, the equation of motion remains as:

$$\sigma_k'' + k^2\sigma_k = 0, \quad (2.74)$$

and the solution is displayed as:

$$\sigma_k(\tau) = \frac{A_1}{\sqrt{2k}}e^{-ik\tau} + \frac{A_2}{\sqrt{2k}}e^{ik\tau}. \quad (2.75)$$

For selecting the initial coefficients  $A_1$  and  $A_2$  it is assumed to start with a vacuum state which minimizes the energy. A possible solution is the Bunch-Davies vacuum<sup>11</sup>. Therefore  $A_1 = 1$  and  $A_2 = 0$ . The final solution is a propagating wave.

- **Wavelength outside the Hubble radius:** the following relation must be achieved:

$$-k\tau \ll 1, \quad (2.76)$$

and the solution will be:

$$\sigma_k(\tau) = B(k)a, \quad (2.77)$$

where  $B(k)$  is a constant of integration. By applying the boundary condition at  $k = aH$  and taking both equations, the constant of integration is defined as:

$$B(k) = \frac{H}{\sqrt{2k^3}}. \quad (2.78)$$

### 2.4.3 Power Spectrum

The power spectrum of an arbitrary quantity  $\chi_k$  is defined as:

$$P_\chi(k) = \frac{k^3}{2\pi^2} |\chi_k|. \quad (2.79)$$

Furthermore, the power spectrum can be constructed as a power law in the following way:

$$P_\chi(k) = A(k_*) \left( \frac{k}{k_*} \right)^{n_\chi - 1}, \quad (2.80)$$

where  $k_*$  is a chosen pivot. The  $n_\chi$  is its associated spectral index that is defined as:

$$n_\chi - 1 = \frac{\ln P_\chi}{d \ln k}, \quad (2.81)$$

where it may be expanded for convenience as:

$$\frac{\ln P_\chi}{d \ln k} = \left( \frac{d \ln P_\chi}{dt} \right) \left( \frac{dt}{d \ln a} \right) \left( \frac{d \ln a}{d \ln k} \right). \quad (2.82)$$

By taking the quantum fluctuation of equation (2.78) and recovering the previous transformation, its power spectrum can be defined as:

$$P_\chi(k) = \frac{k^2}{2\pi^2} \left( \frac{H^2}{2k^3} \right) \rightarrow \left( \frac{H}{2\pi} \right)^2, \quad (2.83)$$

for this special case, as there  $n_\chi$  is equal to 1.

#### 2.4.4 Massless scalar field in quasi-de-Sitter

In a quasi-de-Sitter period, the Hubble radius is not constant anymore. Furthermore, it varies with time and it is described by the slow roll parameter  $\epsilon$  as follows:

$$\dot{H} = -\epsilon H^2. \quad (2.84)$$

Then, it is necessary to compute the new scale factor. After some calculations, the scale factor for not constant Hubble radius in conformal time is:

$$a(\tau) \sim -\frac{1}{H} \left( \frac{1}{\tau^{1+\epsilon}} \right). \quad (2.85)$$

By adding equation (2.85) in (2.86):

$$\sigma_k'' + \left[ k^2 - \frac{1}{\tau^2} \left( \nu^2 - \frac{1}{4} \right) \right] \sigma_k = 0, \quad (2.86)$$

where a expression for  $\nu$  is:

$$\nu^2 - \frac{1}{4} = 2 + 3\epsilon. \quad (2.87)$$

The solution can be written in terms of Hankel's function as follows:

$$\sigma_k(\tau) = \sqrt{\tau} \left[ c_1 H_\nu^{(1)}(-k\tau) + c_2 H_\nu^{(2)}(-k\tau) \right]. \quad (2.88)$$

By applying once again the Buch-Davies vacuum, an approximation of the power spectrum can be read as:

$$\sigma_k(\tau) \sim \frac{1}{\sqrt{2k}} (-k\tau)^{\frac{1}{2}-\nu} \rightarrow (-k\tau)^{\frac{3}{2}-\nu}, \quad (2.89)$$

and by replacing:

$$\nu \approx \frac{3}{2} + \epsilon, \quad (2.90)$$

in equation (2.89):

$$P_\chi(k) \sim \left( \frac{k}{aH} \right)^{-2\epsilon}. \quad (2.91)$$

Therefore, the spectral index for a massless scalar field in a quasi-de Sitter epoch is described by equation (2.91). At quasi-de Sitter,  $\epsilon = 0$  and we recover the classical expression demonstrated in equation (2.83).

### 2.4.5 Scalar and Tensorial modes

The linear evolution of the cosmological perturbations is obtained by perturbing the FRW metric. In a linear order, the scalar, vector, and tensor perturbations evolve independently, and therefore they may be decoupled for analyzing them separately. As vector perturbations do not get excited in the inflationary epoch, there is not possible to compute them. Tensor perturbations or their tensor modes will appear as gravitational waves originated during inflation. Finally, scalar perturbations will be related to the CMB anisotropies.

#### Perturbed equations

The perturbed FRW metric is:

$$g_{\mu\nu} = g_{\mu\nu}^{(o)}(t) + \delta g_{\mu\nu}(x, t), \quad (2.92)$$

Where the Ricci scalar perturbation is:

$$\delta R_{\mu\nu} = \partial_\alpha \delta \Gamma_{\mu\nu}^\alpha - \partial_\mu \delta \Gamma_{\nu\alpha}^\alpha + \delta \Gamma_{\sigma\alpha}^\alpha \Gamma_{\mu\nu}^\sigma + \Gamma_{\sigma\alpha}^\alpha \delta \Gamma_{\mu\nu}^\sigma - \delta \Gamma_{\sigma\nu}^\alpha \Gamma_{\mu\alpha}^\sigma - \Gamma_{\sigma\nu}^\alpha \delta \Gamma_{\mu\alpha}^\sigma, \quad (2.93)$$

and the perturbation of the scalar curvature is:

$$\delta R = \delta g^{\mu\alpha} R_{\alpha\mu} + g^{\mu\alpha} R_{\alpha\mu}. \quad (2.94)$$

The perturbed Einstein tensor is:

$$\delta G_{\mu\nu} = \delta R_{\mu\nu} - \frac{1}{2} \delta g_{\mu\nu} R - \frac{1}{2} g_{\mu\nu} \delta R. \quad (2.95)$$

The perturbation of the stress energy-momentum tensor is defined as:

$$\delta T_{\mu\nu} = \partial_\mu \delta \phi \partial_\nu \phi + \partial_\mu \phi \partial_\nu \delta \phi - \delta g_{\mu\nu} \left( \frac{1}{2} g^{\alpha\beta} \partial_\alpha \phi \partial_\beta \phi + V(\phi) \right) - g_{\mu\nu} \left( \frac{1}{2} g^{\alpha\beta} \partial_\alpha \phi \partial_\beta \phi + g^{\alpha\beta} \partial_\alpha \delta \phi \partial_\beta \phi + 2 \frac{\partial V}{\partial \phi} \delta \phi \right). \quad (2.96)$$

Full calculations were written explicitly by Alexander Riotto<sup>10</sup>.

#### Curvature perturbation

In order to analyze cosmological density perturbations, gauge theory must be considered. General relativity is a gauge theory where a gauge transformation is a coordinate transformation from a local frame to another. Therefore, it is necessary to define physical quantities that may be observable and must be gauge invariant. The perturbation of a given quantity is the difference between its physical value and an unperturbed value in the background (this will be defined with the  $o$  subscript). For making the connection of these two quantities, a gauge choice must be done, which is referred to as a gauge transformation.

The metric for computing the curvature perturbation is:

$$ds^2 = a^2(\tau) \left[ -(1 + 2\Phi) d\tau^2 + (1 - 2\Psi) d\vec{x}^2 \right], \quad (2.97)$$

where the term next to the  $d\tau^2$  is known as the longitudinal gauge or conformal Newtonian gauge and the term corresponding to the space part is the gravitational potential. For computing the quantum fluctuations of the curvature, these two relations will be taken into account:

$$\Psi \rightarrow \Psi + H\delta x^0, \quad (2.98)$$

$$\rho \rightarrow \rho - \dot{\rho}_o \delta x^0. \quad (2.99)$$

Therefore, it is possible to introduce the comoving curvature perturbation:

$$\zeta = \Psi + H \frac{\delta \rho}{\rho_o}, \quad (2.100)$$

which is gauge invariant. It is possible to prove it in the following way:

$$\zeta \rightarrow \tilde{\zeta} = \tilde{\Psi} + H \frac{\delta \tilde{\rho}}{\rho_o}, \quad (2.101)$$

and by using equation (2.98) and (2.99):

$$\tilde{\zeta} = \Psi + H\delta x^o + H \frac{\delta \rho}{\rho_o} - H\delta x^o. \quad (2.102)$$

Then, it can be seen that the initial quantity was recovered. This gauge has two possible forms which are described as follows.

$$\zeta \Big|_{\Psi=0} = \frac{H\delta\rho}{\rho_o} \rightarrow \textit{flat gauge}, \quad (2.103)$$

$$\zeta \Big|_{\delta\rho=0} = \Psi_{\delta\rho=0} \rightarrow \textit{uniform density gauge}. \quad (2.104)$$

For the computing of the density perturbation, it will be used the expression in (2.103). Additionally, it can be obtained another useful gauge invariant which is:

$$R = \Psi + H \frac{\delta \phi}{\dot{\phi}_o}. \quad (2.105)$$

It may be derived from the comoving density perturbation by applying the following conditions:

$$\dot{\rho}_o + 3H(\rho_o + P_o) = 0, \quad (2.106)$$

$$p_o + \rho_o = \dot{\phi}_o^2, \quad (2.107)$$

$$\delta\rho = V' \delta\phi. \quad (2.108)$$

By replacing the previous equations and the slow roll equation from the last part in (2.105),  $\zeta$  takes the form of:

$$S = \Psi + H \frac{\delta \dot{\phi}}{\dot{\phi}_o}. \quad (2.109)$$

Thus, it may be seen that:

$$S \equiv R. \quad (2.110)$$

Once the mathematical tools were proved, it is possible to compute the power spectrum of the comoving curvature perturbation which is related to the density fluctuations. For simplicity, the equivalence in equation (2.105) will be used by applying the condition for the flat gauge. Then:

$$\zeta \Big|_{\Psi=0} = H \frac{\delta\phi}{\dot{\phi}_o}, \quad (2.111)$$

and the power spectrum is written as follows

$$P_\zeta \approx \frac{1}{2M_{pl}^2\epsilon} \left( \frac{H}{2\pi} \right)^2. \quad (2.112)$$

For obtaining the spectral index, it is necessary to solve the following equation:

$$n_\zeta - 1 = \frac{d \ln P_\zeta}{d \ln k}. \quad (2.113)$$

where the final result is:

$$n_\zeta = 1 - 6\epsilon + 2\eta. \quad (2.114)$$

Finally, the full expression for the comoving curvature perturbation for super-Hubble scales written in power law is:

$$P_\zeta = \frac{1}{2M_{pl}^2\epsilon} \left( \frac{H}{2\pi} \right)^2 \left( \frac{k}{aH} \right)^{n_\zeta - 1}. \quad (2.115)$$

### Gravitational waves

As well as scalar perturbations, quantum fluctuations in the gravitational fields are generated in the same way. It can be seen as a ripple of space time in the FRW metric. The action of the tensor perturbation can be written in the following way:

$$S[h] = \frac{M_{pl}^2}{2} \int d^4x \sqrt{-g} \left[ \frac{(h'_{ij})^2}{2} - \frac{(\nabla h_{ij})^2}{2} \right]. \quad (2.116)$$

It can be seen that this action has the same form of the massless scalar field in a quasi-de Sitter space. Therefore, we may write the same result that was obtained. Perturbations are almost frozen on the super-Hubble scales, then we may use the following power spectrum.

$$P_h \approx \frac{8}{M_{pl}^2} \left( \frac{H}{2\pi} \right)^2, \quad (2.117)$$

where the dependence of the tensor spectral index can be approximated by:

$$P_T \sim k^{n_T}. \quad (2.118)$$

Thus, the value of the index is:

$$n_T = -2\epsilon. \quad (2.119)$$

Finally, the power spectrum of the tensor perturbations for super-Hubble scales written as a power law is:

$$P_T = \frac{8}{M_{pl}} \left( \frac{H}{2\pi} \right)^2 \left( \frac{k}{aH} \right)^{n_T}. \quad (2.120)$$

### **Consistency relation**

An intuitive way to analyze the inflationary potential is by using the following relation:

$$r = \frac{P_t}{P_s} = 16\epsilon. \quad (2.121)$$

This quantity may be compared with the one presented in the CMB anisotropies. If the value does not vary much with the experimental data, it implies that the inflation has not been driven for a single field.

# Chapter 3

## Methodology

Once the fundamental theory of the manuscript was defined, it is necessary to compute all quantities by using the desired inflationary potential. The first part is for analyzing the Starobinsky Inflationary Potential, obtained by the Einstein Modified gravity. After that, a new  $f(R)$  variant is introduced which leads to the Generalized Starobinsky Potential, the fundamental equation that will be studied. The second part consists of computing slow-roll parameters for calculating the scalar factor and the scalar field. Finally, in the last part, it is obtained the perturbation equations by using the slow-roll approximation in terms of the previously obtained potential.

### 3.1 Starobinsky Inflation

The first self-consistent model of inflation is  $R^2$  potential, postulated by Alekséi Starobinsky<sup>12</sup> in 1980 where  $R$  is defined as the Ricci Curvature. It was one of the earliest models of inflation that basically considered an additional term in the Einstein-Hilbert action proportional to the squared curvature scalar  $R^2$  as can be seen:

$$S = \frac{M_p^2}{2} \int d^4x \sqrt{-g} \left[ R + \frac{\kappa}{2M_p^2} R^2 \right], \quad (3.1)$$

where  $\kappa$  is a real parameter,  $g$  is determinant of the Friedmann–Lemaître–Robertson–Walker metric and  $M_p$  is the Planck mass<sup>13</sup>. In order to analyze how suitable is this  $f(r)$  it is necessary to perform a Weyl Transformation<sup>14</sup> or conformal transformation on the metric as follows:

$$\bar{g}_{\mu\nu} = \Omega^2 g_{\mu\nu}. \quad (3.2)$$

By taking:

$$\Omega^2 = 1 + \frac{\kappa R}{2M_p^2} = e^{-w}. \quad (3.3)$$

Under this transformation, the Ricci scalar is transformed as

$$\bar{R} = e^{-2w} \left[ R - (2D - 1)\partial^\mu \partial_\mu w - (D - 1)(D - 2)(\partial^\mu w)(\partial_\mu w) \right] \quad (3.4)$$

Where  $D$  = is the space-time dimension. The derivative can be omitted cause is a total derivative. By imposing the scalar field as

$$\phi = M_p \sqrt{\frac{3}{2}} \log \left( 1 + \kappa \frac{R}{M_p^2} \right), \quad (3.5)$$

and by setting  $D = 4$  it is possible to write the transformed scalar in the following form:

$$\bar{R} = e^{-\sqrt{\frac{2}{3}}\phi/M_p} \left[ \frac{M_p^2}{k} (e^{\sqrt{\frac{2}{3}}\phi/M_p} - 1) - \frac{1}{M_p^2} \partial_\mu \phi \partial^\mu \phi \right]. \quad (3.6)$$

By squaring (3.6) and keeping only terms up to second order which can be understand it as no interactions:

$$\bar{R}^2 = \frac{M_p^4}{\kappa^2} (1 - e^{-\sqrt{\frac{2}{3}}\phi/M_p})^2 - \frac{2}{\kappa} \Omega^{-2} g^{\mu\nu} \partial_\mu \phi \partial_\nu \phi + \dots \quad (3.7)$$

Finally, by inserting equation (3.7) into equation (3.1) and writing all in terms of barred quantities is possible to write Einstein modified gravity as follows:

$$S = \frac{M_p^2}{2} \int d^4x \sqrt{-\bar{g}} \left[ \frac{M_p^2}{2} \bar{R} - \frac{1}{2} \bar{\partial}_\mu \phi \bar{\partial}^\mu \phi + \frac{M_p^4}{4\kappa} (1 - e^{-\sqrt{\frac{2}{3}}\phi/M_p})^2 \right]. \quad (3.8)$$

Where the last term in equation (3.8) is the inflationary potential which is:

$$-V(\phi) = \frac{M_p^4}{4\kappa} (1 - e^{-\sqrt{\frac{2}{3}}\phi/M_p})^2. \quad (3.9)$$

Equation (3.9) is known as the Starobinsky Inflationary Potential.

### 3.1.1 Generalized Starobinsky Potential

Several variations of the Starobinsky potential have been analyzed, such as the  $Rpl$  potential<sup>15,16</sup>, the  $R^p$  potential<sup>17</sup>, or even some  $f(r)$  generalizations<sup>18,19</sup>. For this manuscript, it was decided to study one of those that comes from a generalization of the  $f(r)$  by adding a free parameter that can be tuned to obtain better consistency with experimental data. This one is the **Generalized Starobinsky Potential** studied by Renzi et al<sup>20</sup>. This potential, represented as  $R^{2p}$  may be calculated analytically by performing the same calculations presented previously. Starting from the action:

$$S = \frac{M_{pl}^2}{2} \int \sqrt{-g} d^4x f(R), \quad (3.10)$$

$M_{pl}$  is the reduced Plack mass, and  $f(r)$  is an arbitrary function that depends on the Ricci scalar curvature. By performing a conformal transformation:

$$g_{\mu\nu}^E = F(R)g_{\mu\nu}, \quad (3.11)$$

and setting  $F(r)$  as

$$F(R) \equiv f'(R) = e^{\sqrt{\frac{2}{3}}\phi/M_{pl}}. \quad (3.12)$$

Therefore, the action takes the form of:

$$S = \int d^4x \sqrt{-g} \left[ -\frac{M_{pl}^2}{2} R_E + \frac{1}{2} g^{\mu\nu} \partial_\mu \phi \partial_\nu \phi - V(\phi) \right], \quad (3.13)$$

where  $V(\phi)$  is the potential that will be calculated. For this potential, it is imposed the following relation:

$$f(R) = R + \frac{R^{2p}}{(6M^2)^{2p-1}}. \quad (3.14)$$

After some extra steps, the generalized Starobinsky potential  $R^{2p}$  has this structure:

$$V = \underbrace{6 \left( \frac{2p-1}{4p} \right) M_{pl}^2 M^2 \left( \frac{1}{2p} \right)^{\frac{1}{2p-1}}}_{V_0} e^{-2\sqrt{\frac{2}{3}}\frac{\phi}{M_{pl}}} \left( e^{\sqrt{\frac{2}{3}}\frac{\phi}{M_{pl}}} - 1 \right)^{\frac{2p}{2p-1}}, \quad (3.15)$$

where  $p$  is a free parameter that can be tuned, Nevertheless it is necessary to choose a range for the possibles values it can take.

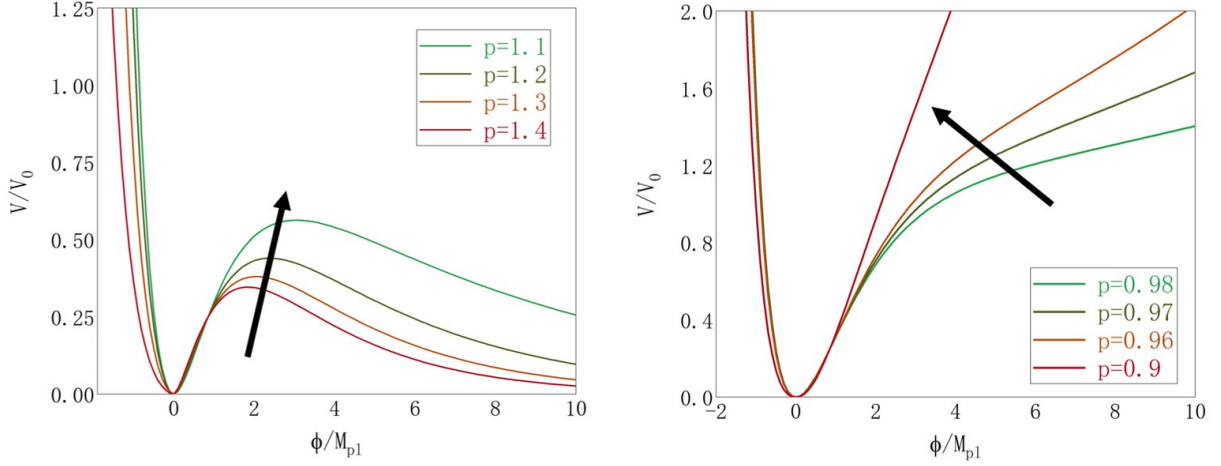


**Figure 3.1:** Generalized Starobinsky Potential for several values of  $p$ . *Left:* Potential evaluated at  $p \geq 1$ , black arrow represents the growth of a maximum. *Right:* Potential evaluated at  $p \leq 1$ . The black arrow represents how only one vacuum is generated. Fig. 3.1a represents the vacuum at the origin while Fig 3.1b represents a possible vacuum when  $\phi/M_{pl}$  tends to positive infinity.

### 3.1.2 Domain of the $p$ -value

The shape of this inflationary potential depends basically on the chosen  $p$  – value. For  $p \leq 1$ , the potential only has one vacuum, which corresponds to the origin. Furthermore, it violates one of the slow-roll conditions. For  $p \geq 1$ , the potential has a maximum located at:

$$\frac{\phi_p}{M_{pl}} = \sqrt{\frac{3}{2}} \ln\left(\frac{2p-1}{p-1}\right). \quad (3.16)$$

For this case, there exist two vacuums. The first one is also located in the origin, while the second one is at  $\phi \rightarrow \infty$ . Therefore, it also violates the slow-roll conditions. Consequently, only small deviations on  $p$  will be considered. Finally, for  $p = 1$ , the potential takes the form of the starobinsky potential. For a better illustration, Figure 3.1 can be seen. For those reasons, it was decided to impose that the possible  $p$ -values than can be taken must be close to one. Therefore, it will be analyzed a smooth deviation of the Starobinsky Potential. These  $p$ -values will be from 0.995 to 1.005. Figure 3.2 shows the values that will be tested in the cosmological observables.

## 3.2 Solving Friedman slow-roll equations

Rewriting equation (2.40) and (2.41) in terms of the scale factor:

$$3 \frac{\dot{a}(t)}{a(t)} \dot{\phi}(t) + V'(\phi(t)) = 0, \quad (3.17)$$

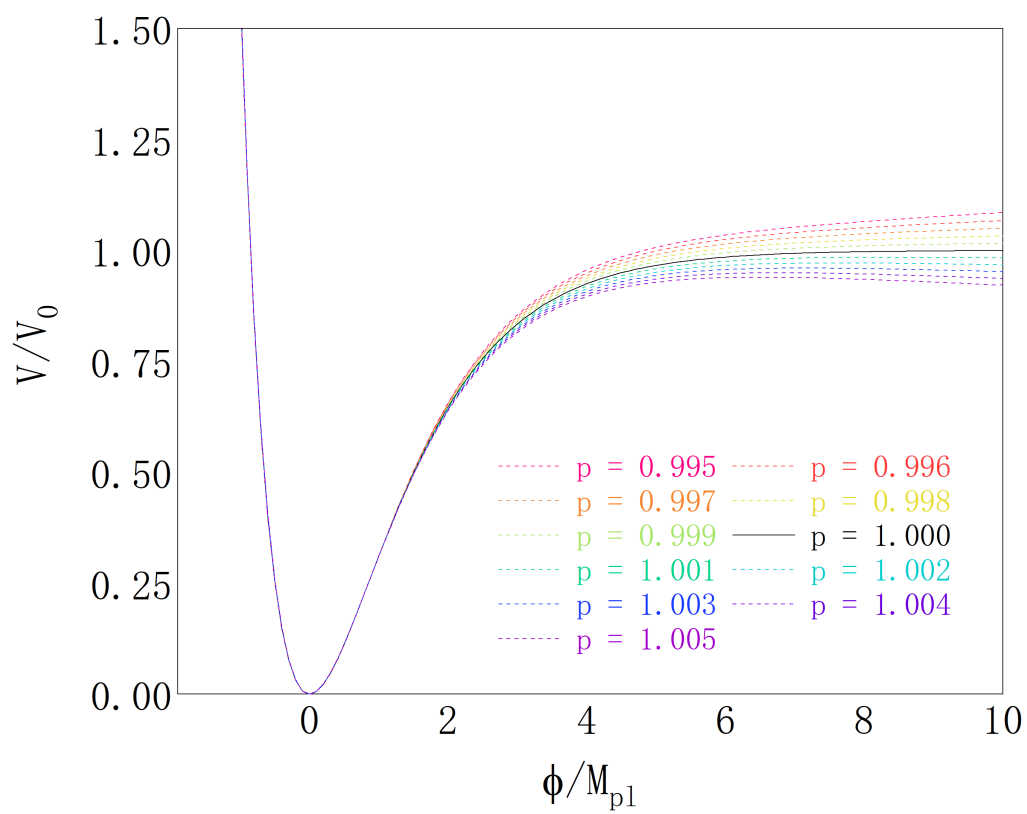


**Figure 3.2:** Generalized Starobinsky Potential. Warm colors represent small values of  $p$  while cold colors symbolize large values of  $p$ . For  $p = 1$ , denoted by the black line, it represents the well-known Starobinsky Potential.

$$a'(t) - a(t) \sqrt{\frac{V'(\phi(t))}{3M_{pl}}} = 0. \quad (3.18)$$

As it may be seen, there are two differential equations of first order, which depend on the scale factor and the scalar field. Therefore two initial conditions are needed. The first one is:

$$a(0) = 1. \quad (3.19)$$

For the second one, it is necessary to compute the scalar field's value at the beginning of the inflation. Thus, rewriting the slow-roll parameters in terms of the chosen potential it is obtained:

$$\epsilon(p, \phi) = \frac{4 \left[ (p-1)e^{\sqrt{\frac{2}{3}}\phi/M_{pl}} - 2p + 1 \right]^2}{3(2p-1)^2 \left( e^{\sqrt{\frac{2}{3}}\phi/M_{pl}} - 1 \right)}, \quad (3.20)$$

$$\delta(p, \phi) = \frac{8(1-p^2) + 8e^2 \sqrt{\frac{2}{3}}\phi/M_{pl} (p-1)^2 - 4e \sqrt{\frac{2}{3}}\phi/M_{pl} (4-13p+10p^2)}{3 \left( -1 + e^{\sqrt{\frac{2}{3}}\phi/M_{pl}} \right)^2 (1-2p)^2}. \quad (3.21)$$

By using the given relation in equation (2.47), compute the scalar field's final value:

$$\epsilon(p, \phi_f) = 1 \rightarrow \phi_f \quad (3.22)$$

Now, using the e-folding number from equation (2.49), two different equations can be obtained:

$$N(p, \phi_i, \phi) = \frac{\sqrt{6}}{4M_{pl}} (\phi - \phi_i) \ln \left[ \frac{1 + e^{\sqrt{\frac{2}{3}}\phi_i/M_{pl}} (p-1) - 2}{1 + e^{\sqrt{\frac{2}{3}}\phi/M_{pl}} (p-1) - 2} \right], \quad (3.23)$$

$$N(1, \phi_i, \phi) = \frac{1}{4} \left[ -3e^{\sqrt{\frac{2}{3}}\phi/M_{pl}} + 3e^{\sqrt{\frac{2}{3}}\phi_i/M_{pl}} + \frac{\sqrt{6}(\phi - \phi_i)}{M_{pl}} \right]. \quad (3.24)$$

Equation (3.23) is used for  $p \neq 1$  while equation (3.24) is for  $p = 1$ . Then by setting  $N$  as the total number of e-folds during inflation, the scalar field's initial value can be computed as follows:

$$N(p, \phi_i, \phi_f) = N \rightarrow \phi_i. \quad (3.25)$$

Equation (3.25) is known as the second initial condition for solving the slow-roll approximation of the Friedman equations.

### 3.2.1 Horizon Crossing

For analyzing the primordial spectrum and their running indexes, the following equation will be used.

$$k = a(t)H(t). \quad (3.26)$$

Where  $k = 0.05$  which is the value where the amplitudes of the perturbations were frozen.

## 3.3 Cosmological Observables

### 3.3.1 Parameters

The previous chapter demonstrated the equations for the scalar power spectrum, tensor power spectrum, spectral index, and tensor-to-scalar ratio by deriving them explicitly from the Einstein-Hilbert action. Nevertheless, it was decided to rewrite those equations more conveniently in terms of the slow-roll parameters and the chosen potential for this section<sup>21,22</sup>. By performing this transformation, these final equations are obtained:

#### Scalar power spectrum

The equation for the primordial scalar power spectrum (2.115) for a general potential is:

$$A_S \simeq \left[ 1 + \frac{25 - 9c}{6}\epsilon - \frac{13 - 3c}{6}\delta \right] \frac{V}{24\pi^2\epsilon}, \quad (3.27)$$

By replacing equations (3.20), (3.21), and (3.15) in (3.27), we obtain the final result:

$$A_S \simeq \left[ 1 + \frac{25 - 9c}{6}\epsilon - \frac{13 - 3c}{6}\delta \right] \frac{1}{24\pi^2\epsilon} V_0 e^{-2\sqrt{\frac{2}{3}}\phi/M_{pl}} \left( e^{\sqrt{\frac{2}{3}}\phi/M_{pl}} - 1 \right)^{\frac{2p}{2p-1}}. \quad (3.28)$$

For convenience with the experimental data, it is necessary to use the following relation:

$$\ln[10^{10}A_S], \quad (3.29)$$

this new quantity is the one reported by the experimental sources, which will be explained later.

#### Scalar spectral index

The final equation for the spectral index can be obtained by replacing the slow-roll parameters and the potential in equation (2.114) as follows.

$$n_S = 1 - 6 \frac{4 \left[ (p-1)e^{\sqrt{\frac{2}{3}}\phi/M_{pl}} - 2p + 1 \right]^2}{3(2p-1)^2 \left( e^{\sqrt{\frac{2}{3}}\phi/M_{pl}} - 1 \right)} + 2 \frac{8(1-p^2) + 8e^2 \sqrt{\frac{2}{3}}\phi/M_{pl} (p-1)^2 - 4e \sqrt{\frac{2}{3}}\phi/M_{pl} (4-13p+10p^2)}{3 \left( -1 + e^{\sqrt{\frac{2}{3}}\phi/M_{pl}} \right)^2 (1-2p)^2}. \quad (3.30)$$

### Tensor power spectrum

The final equation for the tensor power spectrum (2.120) for a general potential is:

$$P_T \simeq \left[ 1 + \frac{1+3c}{6} \epsilon \right] \frac{2V}{3\pi^2}. \quad (3.31)$$

By replacing equation (3.20), (3.21) and (3.15) in the last relation, it is possible to obtain:

$$P_T \simeq \left\{ 1 + \frac{1+3c}{6} \frac{4 \left[ (p-1)e^{\sqrt{\frac{2}{3}}\phi/M_{pl}} - 2p + 1 \right]^2}{3(2p-1)^2 \left( e^{\sqrt{\frac{2}{3}}\phi/M_{pl}} - 1 \right)} \right\} \frac{2}{3\pi^2} V_0 e^{-2\sqrt{\frac{2}{3}}\phi/M_{pl}} \left( e^{\sqrt{\frac{2}{3}}\phi/M_{pl}} - 1 \right)^{\frac{2p}{2p-1}} \quad (3.32)$$

### Tensor spectral index

By replacing in equation (2.119) the slow roll parameter  $\epsilon$ :

$$n_T = -2 \frac{4 \left[ (p-1)e^{\sqrt{\frac{2}{3}}\phi/M_{pl}} - 2p + 1 \right]^2}{3(2p-1)^2 \left( e^{\sqrt{\frac{2}{3}}\phi/M_{pl}} - 1 \right)} \quad (3.33)$$

### Tensor-to-scalar ratio

Finally, the tensor-to-scalar (2.121) ratio can be computed as:

$$r = 16 \frac{4 \left[ (p-1)e^{\sqrt{\frac{2}{3}}\phi/M_{pl}} - 2p + 1 \right]^2}{3(2p-1)^2 \left( e^{\sqrt{\frac{2}{3}}\phi/M_{pl}} - 1 \right)} \quad (3.34)$$

## 3.3.2 Experimental observations

To analyze how accurate the generalized Starobinsky potential, it is necessary to compare the theoretically obtained results with the experimental values that may be found in the literature. Therefore, the values of the cosmological parameters that will be considered for this manuscript are described in Table 3.1 .

Parameters	Starobinsky inflation
$A_S$	$2.21093 \times 10^{-9}$
$\ln(10^{10}A_S)$	3.096
$n_S$	0.9656
$r$	0.00363

**Table 3.1:** Experimental values of the Cosmological observables.  $A_S$  is the scalar power spectrum,  $n_S$  is its spectral index,  $r$  is defined as the scalar-to-tensor ratio and the  $\ln 10^{10}A_S$  is a more convenient way for describing the scalar power spectrum. Those values are taken from Planck 2018.



# Chapter 4

## Results & Discussion

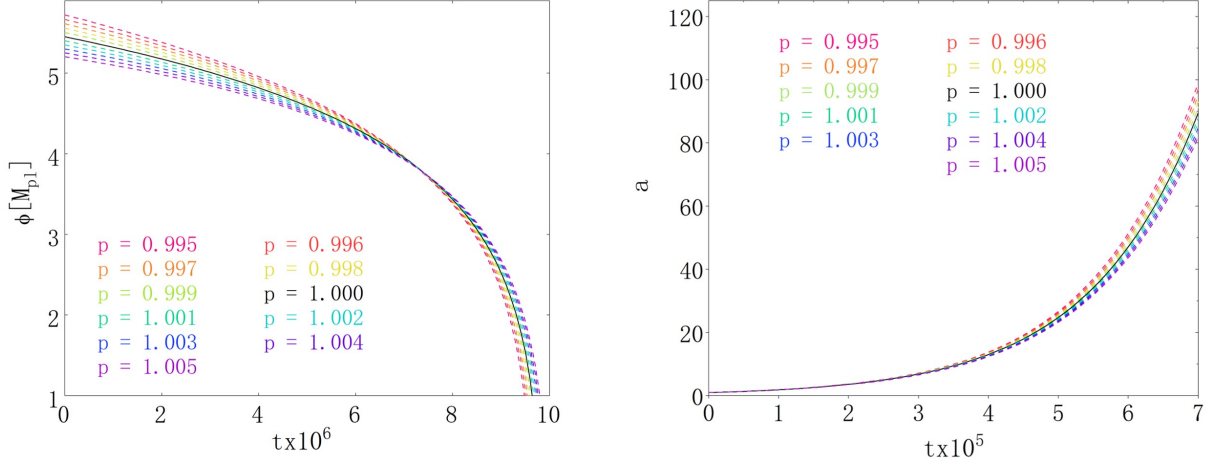
This section consists of the numerical calculations of the equations in the last chapter. The first part is dedicated to computing the scale factor and the scalar field by using the Friedman Equation's slow-roll approximation. Secondly, the following part is computing the scalar power spectrum and the scalar spectral index with the slow-roll approximation. Those results will be compared with the ones reported in Planck 2018, and a final value of the  $p$ -value will be obtained. Finally, the last part focuses on analyzing the tensor power spectrum, its Spectral Index, and the tensor-to-scalar Ratio using the previously obtained  $p$ -value. At the end of the chapter, a set of cosmological parameters will be reported.

### 4.1 Scalar field and Scale factor

Calculation of the scalar field and the scale factor can be displayed by solving equations (3.17) and (3.18). Additionally, both equations were solved coupled, and it is needed to compute first the initial parameters. The initial value of the scalar field can be obtained by solving equation (3.23). Moreover, for the special case of  $p = 1$ , equation (3.24) must be used instead. Explicit results can be found in Table 4.1. For the scale factor's initial value,  $a(0) = 1$  was set. The number of folding was set at  $N = 60$ , the mass value was taken as  $M = 130/10^7$  and the Reduced Planck mass value was set as  $M_{pl} = 1$ . Both equations were solved for a set of  $p$  values, from 0.995 to 1.005, increasing 0.001 units.

$p$	<b>0.995</b>	<b>0.996</b>	<b>0.997</b>	<b>0.998</b>	<b>0.999</b>	<b>1.000</b>	<b>1.001</b>	<b>1.002</b>	<b>1.003</b>	<b>1.004</b>	<b>1.005</b>
$\phi_o$	5.724	5.668	5.613	5.558	5.505	5.454	5.401	5.351	5.301	5.252	5.204
$\phi_f$	0.9473	0.9458	0.9444	0.9430	0.9415	0.9491	0.9387	0.9373	0.9359	0.9345	0.933

**Table 4.1:** Initial  $\phi_0$  and final  $\phi_f$  values of the scalar field in the inflationary epoch for different values of  $p$ .



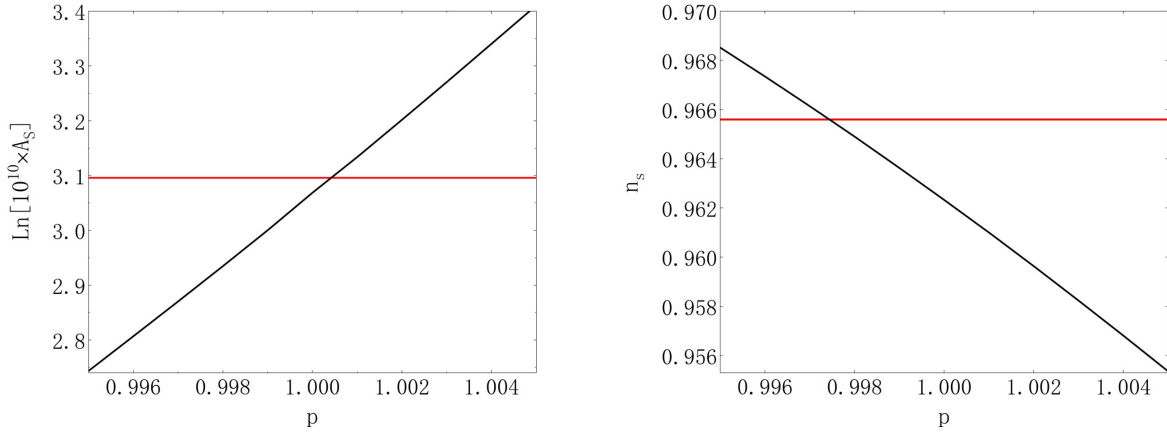
**Figure 4.1:** *Left:* Time evolution of the scalar field during the inflationary epoch. *Right:* Time evolution of the scale factor. For both graphs, different values of  $p$  are displayed.

Figure 4.1 (left) shows the scalar field's time evolution for a discrete range of  $p$ -values. Oscillation of the scalar field is only visible if a full calculation is performed. On the other side, Figure 4.1 (right) shows the dynamics of the scale factor, consistent with the information reported in the literature. An exponential expansion takes place during the inflationary epoch. Similarly, it is shown its behavior by using several values of  $p$ . For both graphics, warm colors represent small values of  $p$  while cold colors symbolize large values of  $p$ . For  $p = 1$ , denoted by the black line, it represents the well-known Starobinsky Potential. It is important to notice that these slight changes of  $p$  vary a few. Nevertheless, they become more fundamental at computing the cosmological observables.

## 4.2 Scalar power spectrum and spectral index

Once the scale factor and the scalar field were obtained, it is possible to compute the Scalar Power Spectrum. For doing this, equation (3.28) is solved by using the set of  $p$  values. For all the cosmological observables that will be obtained, equation (3.26) is used by setting  $k = 0.05$ . For convenience, equation (3.29) is used to obtain the  $\ln(10^{10}A_S)$  which are the generic values reported in the literature. Therefore, it will be possible to compare the accuracy of the computed values with the experimental values. For the scalar spectral index, equation (3.30) is solved for different values of  $p$ . Similarly, obtained values are also compared with the reported ones.

Figure 4.2 (left) shows the behavior of the  $\ln(10^{10}A_S)$  for  $p$  from 0.995 to 1.005. Red line represents the experimental value reported by Planck 2018, which is 3.096. It may be seen that near from  $p = 1$ , both values coincide. This makes sense since, we recover the Starobinsky potential. Values of the  $\ln(10^{10}A_S)$  get higher as  $p$  increases. Scalar spectral index is plotted in Figure 4.2 (right) for the same values of  $p$ .



**Figure 4.2:** Behaviour of the cosmological observables with respect of different values of  $p$  at  $k = 0.05$ . *Left:*  $\ln(10^{10}A_s)$ . *Right:* Scalar spectral index.

<b>p</b>	<b>0.995</b>	<b>0.996</b>	<b>0.997</b>	<b>0.998</b>	<b>0.999</b>	<b>1.000</b>	<b>1.001</b>	<b>1.002</b>	<b>1.003</b>	<b>1.004</b>	<b>1.005</b>
(a)	1.5548	1.6556	1.7646	1.8824	2.0098	2.151	2.2969	2.4586	2.6339	2.8241	3.0301
(b)	2.7439	2.8068	2.8705	2.9351	3.000	3.0686	3.1341	3.2022	3.2710	3.3407	3.4111
(c)	0.9685	0.9673	0.9661	0.9649	0.963	0.9626	0.9609	0.9596	0.9582	0.9568	0.9553

**Table 4.2:** Computed values of the cosmological observables: (a) Scalar Power Spectrum  $A_s$ , (b)  $\ln(10^{10}A_s)$ , (c) and its spectral index ( $n_s$ ).

Similar; the red line shows the experimental value obtained in literature which is  $n_s = 0.9656$ , reported by Planck 2018. In contrast with the previous result, the index decreases when  $p$  increases. Both sets of values are reported in Table 4.2. Red values represent the inferior and superior limit of the observables previously explained. It is fundamental to choose in which parameter we want the higher accuracy. For this manuscript, we decided to focus on the Scalar power spectrum, or as it has been reported here,  $\ln(10^{10}A_s)$ .

<b>p</b>	<b>1.0003</b>	<b>1.0004</b>	<b>1.0005</b>	<b>1.0006</b>	<b>1.0007</b>
$\ln(10^{10}A_s)$	3.08705	3.09376	3.10047	3.1072	3.11393
$A_s(x10^{-9})$	2.19124	2.20598	2.22085	2.23583	2.25093

**Table 4.3:** Computed values of the cosmological observables  $A_s$  and  $\ln(10^{10}A_s)$  from  $p = 0.0003$  to  $p = 0.0007$  at  $k = 0.05$ .

For obtaining a better accuracy for  $p$ , its interval value is decreased up to 0.0001. Figure 4.3 shows a zoom of the  $\ln(10^{10}A_s)$ . Data can be seen closely in table 3. From these, it was decided that the optimal value of  $p$  for having a high accuracy for our cosmological observable is  $p = 1.0004$ . Described values are shown in Table 4.3. It is important to clarify that it was possible to add more decimals in order to obtain better results, but for this manuscript,

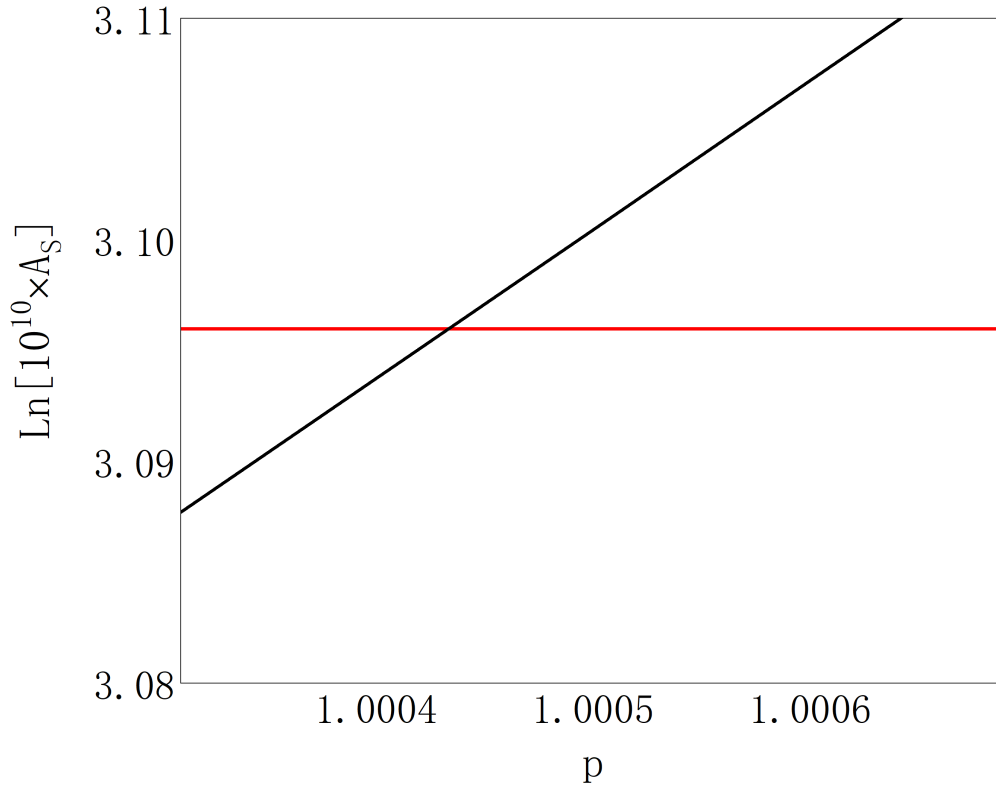


**Figure 4.3:** Deeper view of the  $\text{Ln}(10^{10}A_s)$  from  $p = 1.0003$  to  $p = 1.0007$  at  $k = 0.05$ .

we decided to stop in four decimals.

Figure 4.4 (left) shows the dynamics of the Scalar Power Spectrum of the Generalized Starobinsky Potential for different values of  $k$ . For this analysis, it was taken the previously computed values in equation (3.26). Figure 4.4 (right) displays the behavior of the Scalar Spectral Index for the same value of  $p$ . In both graphs, the red dot refers to the final computed value at  $p = 1.004$  and  $k = 0.05$ .

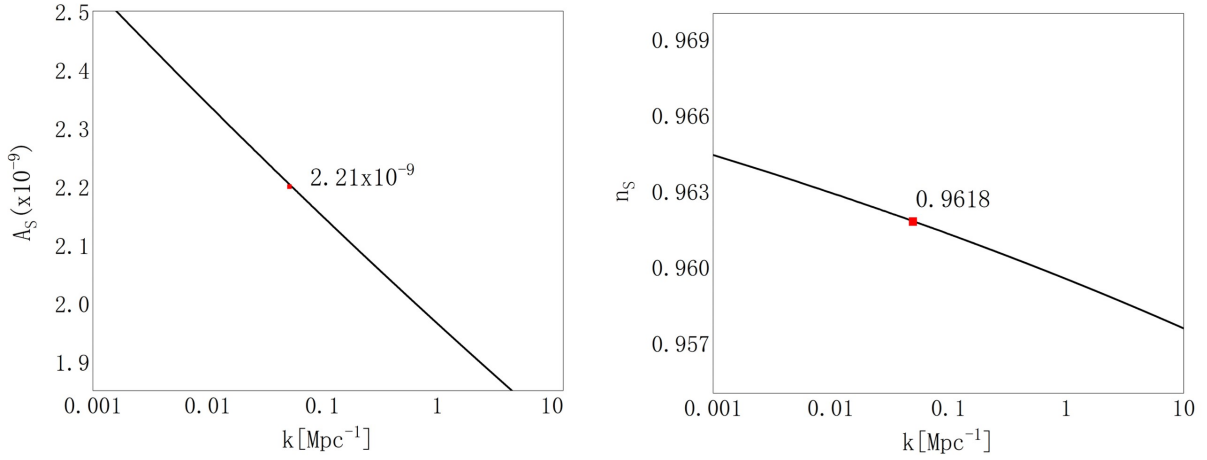


**Figure 4.4:** Dynamics of the cosmological observables for  $p = 1.0004$  at different values of  $k$ . *Left:* Scalar Power Spectrum. *Right:* Scalar Spectral Index. Red dots describes the values at  $k = 0.05$ .

### 4.3 Tensor Power Spectrum, Spectral Index and Tensor-to-scalar Ratio

In Figure 4.5 is presented three different plots. The left one is the tensor power spectrum (3.32), the right one is the tensor-to-scalar ratio (3.34), and the one at the bottom is the tensor spectral index (3.33). All graphics were computed at  $k = 0.05$  and for different values of  $p$ . This was made to analyze the behavior of the cosmological parameters when  $p$  varies slightly. For the tensor power spectrum and its spectral index, the same tendency is observed, a decreasing of those values at large values of  $p$ . In contrast, by analyzing the tensor-to-scalar ratio, it increases its magnitude when  $p$  increases too. Explicit values can be found in Table 4.4 .

$p$	0.995	0.996	0.997	0.998	0.999	1.000	1.001	1.002	1.003	1.004	1.005
$P_t$	8.6964	8.6190	8.5438	8.4707	8.3997	8.3307	8.2632	8.1978	8.1340	8.07199	8.0115
$n_t$	-7.220	-6.728	-6.265	-5.831	-5.423	-5.031	-4.681	-4.344	-4.029	-3.735	-3.460
$r$	0.0057	0.0053	0.0050	0.0046	0.0043	0.0040	0.0037	0.0034	0.0032	0.0029	0.0027

**Table 4.4:** Computed values of the cosmological observables  $P_T$ ,  $n_T$  and  $r$  for several values of  $p$  at  $k = 0.05$ .

As the  $p$  – value was already found, it is now represented, in Figure 4.6, the dynamics of the three cosmological parameters concerning  $k$  for the Generalized Starobinsky Potential at  $p = 1.004$ . Similarly, the red dot represents the computed value of the parameters at  $k = 0.05$ .

Numerical value of the tensor power spectrum has a very good approximation with the value reported in the literature<sup>23</sup>. In addition, the scalar-to-tensor ratio coincides with the values reported in Planck 2018.

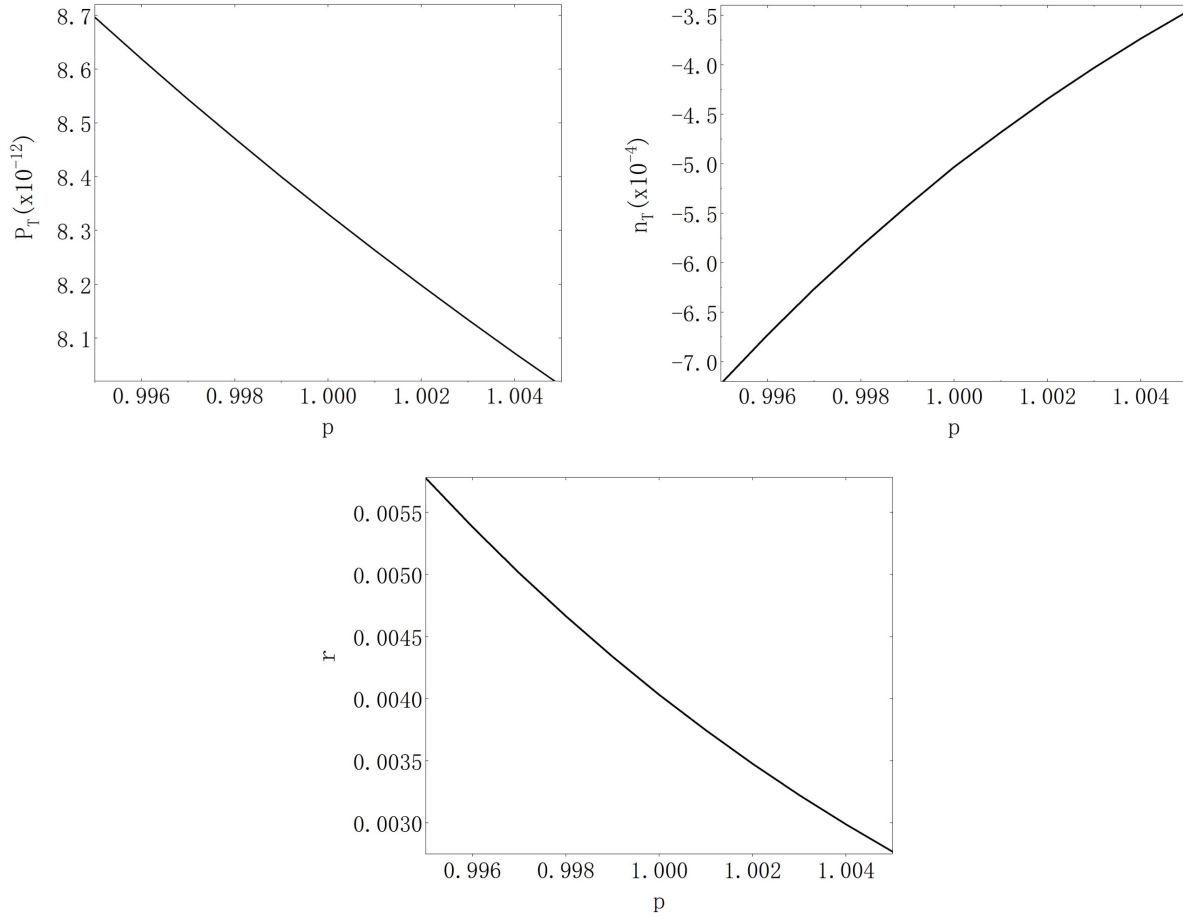


**Figure 4.5:** Behaviour of the cosmological observables for different values of  $p$  at  $k = 0.05$ . *Left:* tensor power spectrum. *Right:* tensor-to-scalar ratio. *Bottom:* tensor Spectral Index.

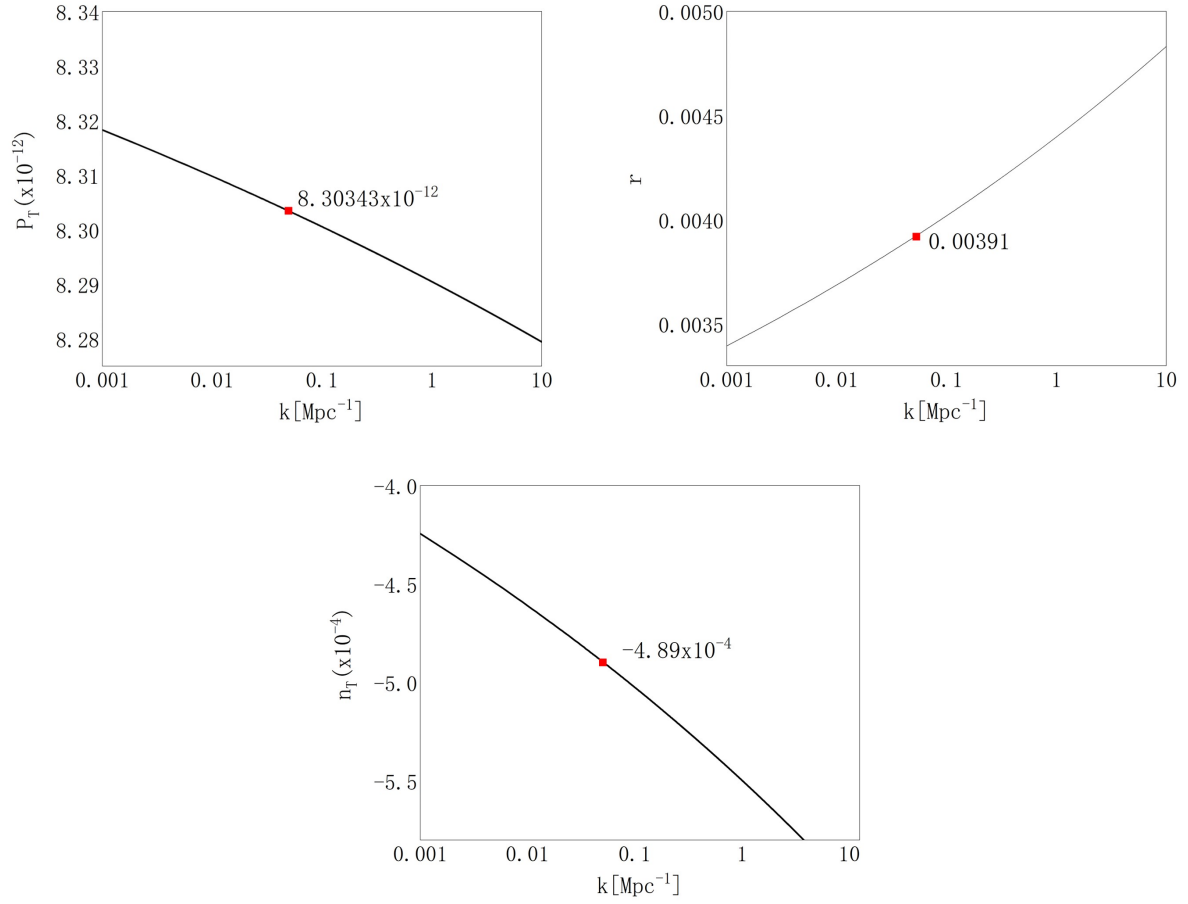


**Figure 4.6:** Dynamics of the cosmological observables for  $p = 1.0004$  at different values of  $k$ . *Left:* Tensor Power Spectrum. *Right:* Tensor-to-scalar ratio. *Bottom:* Tensor Spectral Index. Red dots describes the values at  $k = 0.05$ .

Finally, it is concluded that the final set of cosmological parameters, including scalar power spectrum, scalar power spectrum amplitude, scalar spectral index, tensor power spectrum, tensor spectral index, and tensor-to-scalar ratio, are in good agreement with the ones reported in the literature. For a final comparison, those are displayed in Table 3.1. It can be seen that the obtained values are consistent with the ones reported by Planck 2018.

Parameters	Computed with $p = 1.0004$	Observational data
$A_S$	$2.20598 \times 10^{-9}$	$2.21093 \times 10^{-9}$
$\ln(10^{10} A_S)$	3.09376	3.096
$n_S$	0.9618	0.9656
$P_T$	$8.30343 \times 10^{-12}$	—
$n_T$	-0.0004893	—
$r$	0.00391	0.00363

**Table 4.5:** Set of cosmological observables using computed at  $p = 1.004$  by using the Generalized Starobinsky Potential and the experimental values reported in Plank 2018.

## Chapter 5

# Conclusions & Outlook

The main objective of this manuscript was to introduce inflationary cosmology as a successful solution for the shortcomings of the Big Bang Standard Cosmology. The flatness problem and Horizon problem are solved by defining a scalar field, which will behave as an ideal fluid thus it mimics a cosmological constant. Furthermore, it is possible to explain the formation of large structures and the anisotropies of CMB by using cosmological perturbation theory as the theoretical framework. Starting from the most basic case, perturbation of a massless scalar field in De Sitter, then it can be obtained the equations that describe the scalar and tensor perturbations during the inflationary epoch. By using approximations it was derived the scalar power spectrum  $A_s$ , tensor power spectrum  $P_t$ , their respective spectral indexes  $n_s, n_t$ , and the scalar-to-ratio tensor  $r$  in the slow-roll approximation for an arbitrary potential.

Using the Generalized Starobinsky Potential  $V(\phi, p)$  that can be computed from the Einstein modified gravity, it is possible to mimic the well-known Starobinsky inflation  $V(\phi, 1)$  and obtain better accuracy concerning the experimental data shown in Table 3.1. Specially, a better approximation for the scalar power spectrum which was obtained by setting  $p = 1.004$ .

One interesting analysis that could be applied in the future is to perform different calculations where the number of e-folds  $N$ , and the mass  $M$  are not fixed. Thus, a better accuracy could be obtained for different cosmological observables.



# Bibliography

- [1] Aghanim, N.; Akrami, Y.; Arroja, F.; Ashdown, M.; Aumont, J.; Baccigalupi, C.; Ballardini, M.; Banday, A. J.; Barreiro, R. B.; et al., Planck2018 results. *Astronomy Astrophysics* **2020**, *641*, A1.
- [2] Baumann, D. Cosmological inflation: Theory and observations. *Advanced Science Letters* **2009**, *2*, 105–120.
- [3] Vazquez Gonzalez, J. A.; Padilla, L. E.; Matos, T. Inflationary cosmology: from theory to observations. *Revista Mexicana de Física E* **2020**, *17*, 73.
- [4] Brandenberger, R. H. *Large Scale Structure Formation*; Springer, 2000; pp 169–211.
- [5] Roos, M. *Introduction to cosmology*; John Wiley & Sons, 2015.
- [6] Brevik, I.; Grøn, Ø.; de Haro, J.; Odintsov, S. D.; Saridakis, E. N. Viscous cosmology for early-and late-time universe. *International Journal of Modern Physics D* **2017**, *26*, 1730024.
- [7] Brawer, R. Inflationary cosmology and horizon and flatness problems: the mutual constitution of explanation and questions. Ph.D. thesis, Massachusetts Institute of Technology, 1995.
- [8] Baumann, D. TASI Lectures on Inflation. 2009.
- [9] Liddle, A. R.; Lyth, D. H. *Cosmological inflation and large-scale structure*; Cambridge university press, 2000.
- [10] Riotto, A. Inflation and the Theory of Cosmological Perturbations. 2002.
- [11] Armendariz-Picon, C. Why should primordial perturbations be in a vacuum state? *Journal of Cosmology and Astroparticle Physics* **2007**, *2007*, 031.
- [12] Starobinsky, A. A. A new type of isotropic cosmological models without singularity. *Physics Letters B* **1980**, *91*, 99–102.
- [13] Roupec, C. O. dS Vacua and Starobinsky Inflation in 4d  $N=1$  Supergravity. Ph.D. thesis, uniwienn, 2017.
- [14] Carneiro, D. F.; Freiras, E. A.; Gonçalves, B.; de Lima, A. G.; Shapiro, I. L. On Useful Conformal Transformations In General Relativity. 2004.
- [15] Martin, J.; Ringeval, C.; Vennin, V. Encyclopædia inflationaris. *Physics of the Dark Universe* **2014**, *5*, 75–235.

- 
- [16] Martin, J.; Ringeval, C.; Trota, R.; Vennin, V. The best inflationary models after Planck. *Journal of Cosmology and Astroparticle Physics* **2014**, 2014, 039.
- [17] Motohashi, H. Consistency relation for  $R_p$  inflation. *Physical Review D* **2015**, 91, 064016.
- [18] Mishra, S. S.; Müller, D.; Toporensky, A. V. Generality of Starobinsky and Higgs inflation in the Jordan frame. *Physical Review D* **2020**, 102, 063523.
- [19] Canko, D. D.; Gialamas, I. D.; Kodaxis, G. P. A simple  $F(R, \phi)$   $F(R, \phi)$  deformation of Starobinsky inflationary model. *The European Physical Journal C* **2020**, 80, 1–13.
- [20] Renzi, F.; Shokri, M.; Melchiorri, A. What is the amplitude of the gravitational waves background expected in the Starobinsky model? *Physics of the Dark Universe* **2020**, 27, 100450.
- [21] Huang, Q.-G. Slow-roll reconstruction for running spectral index. *Physical Review D* **2007**, 76, 043505.
- [22] Stewart, E. D.; Lyth, D. H. A more accurate analytic calculation of the spectrum of cosmological perturbations produced during inflation. *Physics Letters B* **1993**, 302, 171–175.
- [23] Rojas, C.; Villalba, V. M. Computation of inflationary cosmological perturbations in chaotic inflationary scenarios using the phase-integral method. *Physical Review D* **2009**, 79, 103502.